Pressure-driven flow of a Herschel-Bulkley fluid with pressure-dependent rheological parameters

Pandelitsa Panaseti,[1] Yiolanda Damianou,[1] Georgios C. Georgiou,[1,a)] and Kostas D. Housiadas[2]
[1]*Department of Mathematics and Statistics, University of Cyprus, P. O. Box 20537, 1678 Nicosia, Cyprus*
[2]*Department of Mathematics, University of the Aegean, Karlovasi 83200, Samos, Greece*

(Received 31 August 2017; accepted 27 September 2017; published online 8 February 2018)

The lubrication flow of a Herschel-Bulkley fluid in a symmetric long channel of varying width, $2h(x)$, is modeled extending the approach proposed by Fusi *et al.* ["Pressure-driven lubrication flow of a Bingham fluid in a channel: A novel approach," J. Non-Newtonian Fluid Mech. **221**, 66–75 (2015)] for a Bingham plastic. Moreover, both the consistency index and the yield stress are assumed to be pressure-dependent. Under the lubrication approximation, the pressure at zero order depends only on x and the semi-width of the unyielded core is found to be given by $\sigma(x) = -(1 + 1/n)h(x) + C$, where n is the power-law exponent and the constant C depends on the Bingham number and the consistency-index and yield-stress growth numbers. Hence, in a channel of constant width, the width of the unyielded core is also constant, despite the pressure dependence of the yield stress, and the pressure distribution is not affected by the yield-stress function. With the present model, the pressure is calculated numerically solving an integro-differential equation and then the position of the yield surface and the two velocity components are computed using analytical expressions. Some analytical solutions are also derived for channels of constant and linearly varying widths. The lubrication solutions for other geometries are calculated numerically. The implications of the pressure-dependence of the material parameters and the limitations of the method are discussed. *Published by AIP Publishing.*
https://doi.org/10.1063/1.5002650

I. INTRODUCTION

Yield-stress fluids, also known as viscoplastic fluids, are encountered in a variety of industrial applications, such as oil drilling and transport, fresh concrete manufacturing, waste management, and food processing, and in many environmental, geological, and biological processes.[1,2] Viscoplastic materials are commonly assumed to behave as fluids only if the stress exceeds the yield stress τ_y^*; otherwise, they behave as solids. (It should be noted that throughout this paper, symbols with stars denote dimensional quantities.) For an update on the ongoing debate about the concept of a yield-stress fluid and the definition of yield stress, the reader is referred to the recent reviews by Malkin *et al.*[3] and by Dinkgreve *et al.*[4] As noted by Coussot *et al.*,[5] most researchers now consider that the yield stress marks a limit between the existence of steady-state flows—above the yield stress—and the observation of continuously slowed down flows.

The most popular constitutive equation describing viscoplastic behavior is the Bingham-plastic equation.[6] This involves two material parameters, i.e., the yield stress and the plastic viscosity μ^*, and has the following tensorial form:

$$\begin{cases} \mathbf{D}^* = \mathbf{0}, & \tau^* \le \tau_y^* \\ \boldsymbol{\tau}^* = 2\left(\frac{\tau_y^*}{\dot\gamma^*} + \mu^*\right)\mathbf{D}^*, & \tau^* > \tau_y^* \end{cases}, \tag{1}$$

where $\boldsymbol{\tau}^*$ is the viscous stress tensor,

$$\mathbf{D}^* \equiv \frac{1}{2}\left[\nabla^*\mathbf{v}^* + (\nabla^*\mathbf{v}^*)^T\right] \tag{2}$$

is the rate of deformation tensor, $\mathbf{v}^*$ is the velocity vector, and $\dot\gamma^* \equiv \sqrt{\mathrm{tr}\mathbf{D}^{*2}/2}$ and $\tau^* \equiv \sqrt{\mathrm{tr}\boldsymbol{\tau}^{*2}/2}$ are the magnitudes of $2\mathbf{D}^*$ and $\boldsymbol{\tau}^*$, respectively. Setting $\tau_y^* = 0$, the Bingham plastic is reduced to the Newtonian constitutive equation and μ^* is simply the familiar Newtonian viscosity. A generalization of the Bingham-plastic equation is the Herschel-Bulkley model,[7] which involves three material parameters,

$$\begin{cases} \mathbf{D}^* = \mathbf{0}, & \tau^* \le \tau_y^* \\ \boldsymbol{\tau}^* = 2\left(\frac{\tau_y^*}{\dot\gamma^*} + k^*\dot\gamma^{*n-1}\right)\mathbf{D}^*, & \tau^* > \tau_y^* \end{cases}, \tag{3}$$

where k^* is the consistency index and n is the flow index (power-law exponent). Setting the latter to unity yields the Bingham-plastic model. Setting $\tau_y^* = 0$ results in the power-law model, which is able to account for shear-thinning ($n < 1$) and shear-thickening ($n > 1$) effects.

Due to the two-branch nature of viscoplastic constitutive equations, the flow domain consists of yielded regions (viscous domain) where $\tau^* > \tau_y^*$ and unyielded regions (rigid domain) where $\tau^* \le \tau_y^*$. The latter regions include stagnant zones where the velocity is zero and zones where the material moves as a solid body. The location of the interface between yielded and unyielded regions is not known *a priori* and causes severe difficulties in solving viscoplastic flows, especially in two and three dimensions.[8]

a)Author to whom correspondence should be addressed: georgios@ucy.ac.cy. Tel.: +357292612. Fax: +35722895352.

The effects of the dependence of the rheological parameters on the pressure are of interest in the present work. The idea of a fluid with pressure-dependent viscosity was introduced by Stokes.[9] Much later, Barus proposed an exponential isothermal equation of state for the Newtonian viscosity of the form[10]

$$\eta^*(p^*) = \eta_0^* \exp\left[\alpha^*(p^* - p_0^*)\right], \tag{4}$$

where p^* is the pressure, η_0^* is the viscosity at the reference pressure p_0^*, and α^* is the viscosity growth or piezoviscous coefficient, which is positive, $\alpha^* \geq 0$. Equation (4) indicates that the viscosity increases with pressure. As noted by Rajagopal[11] the dependence of the viscosity on pressure for fluids like polymer melts and lubricants may be several orders of magnitude stronger than that of density, which justifies the study of incompressible flows with pressure-dependent viscosity. The pressure-dependence of the viscosity becomes important in high-pressure processes, such as polymer processing, fluid film lubrication, microfluidics, and geophysics (see Ref. 12 and the references therein). Goubert *et al.* reviewed measurement techniques for evaluating the pressure dependence of viscosity.[13] The viscosity growth coefficient is typically 1-5 $\times 10^{-8}$ Pa^{-1} for polymer melts,[14] 1-2 $\times 10^{-8}$ Pa^{-1} for mineral oils,[15] and 2-5 $\times 10^{-8}$ Pa^{-1} for heavy petroleum fractions.[16]

Other equations describing the pressure-dependence of the viscosity have also been proposed. For more information, the reader is referred to the review paper of Málek and Rajagopal.[17] The linear equation

$$\eta^*(p^*) = \eta_0^*\left[1 + \alpha^*(p^* - p_0^*)\right], \tag{5}$$

which has also been used by various investigators,[12,18] is essentially the approximation of the Barus equation (4) at low pressures and/or for low values of the viscosity growth coefficient. A source of major concern with Eq. (5) is the fact that it does not guarantee positive definiteness of the viscosity which requires the pressure to remain positive.[19] This limitation is not encountered when using the Barus equation (4) or in flows where the pressure difference remains positive, e.g., in Poiseuille flows.[12]

The effect of pressure has also been studied in the case of non-Newtonian materials. For example, Laun proposed the following Barus-type equation for the consistency index of LDPE (low-density polyethylene) melts:[20]

$$k^*(p^*, T^*) = k_0^* \exp\left[\alpha^*(p^* - p_0^*) - \gamma^*(T^* - T_0^*)\right], \tag{6}$$

where T^* is the temperature, T_0^* is the reference temperature, and γ^* is the temperature coefficient. Hermoso *et al.*[21] presented experimental viscosity data for shear thinning (non-viscoplastic) oil-based drilling fluids, which show that the viscosity follows a Sisko-Barus (i.e., with an exponential growth term) model in which the consistency and flow indices also vary linearly with pressure. The rheological behavior of drilling fluids is greatly affected by the temperature and pressure conditions and plays an important role in the bottom-hole pressure occurring in deep hot wells.[22] Ibeh reported viscometric data on various drilling fluids suggesting linear and exponential variations of the viscosity with pressure and temperature, respectively.[23] He also pointed out that the effects of temperature on the viscosity prevail at higher pressures, while pressure effects become more pronounced at lower temperatures.

The pressure-dependence of the yield stress is well established in the mechanics of solid and granular materials (see Ref. 24 and the references therein). The pressure- as well as the temperature-dependence of the rheological parameters has also been the subject of various experimental studies on other viscoplastic materials, especially in the oil and gas industry, e.g., in transport operations design[25] and in oil drilling, given the high pressures and temperatures encountered in the wells.[22]

Politte proposed a seven-parameter empirical expression for the plastic viscosity of certain drilling fluids as a function of both temperature and pressure.[26] He reported that the yield stress is not a strong function of pressure and becomes even weaker as temperature increases. Houwen and Geehan proposed a simple four-parameter model to determine both the yield stress and the high-shear-rate viscosity of invert muds as a function of pressure and temperature.[27] Hermoso *et al.* investigated the combined effects of pressure and temperature on the rheological behavior of two oil-based drilling fluids and found that this is described fairly well with the Bingham-plastic or the Herschel-Bulkley models.[28] In the range of their experimental conditions, the power-law exponent was practically unaffected and the yield stress decreased linearly with temperature and increased linearly with pressure. A similar trend has also been observed in the experiments of Ibeh[23] on oil-based drilling fluids at ultra-high pressures and temperatures. Hermoso *et al.* suggested that the increase in yield stress with pressure is associated with the compression effect of different resulting organoclay microstructures.[28] In order to model the isothermal yield stress behavior of the two drilling fluids, they employed the following linear equation:[28]

$$\tau_y^*(p^*) = \tau_0^*\left[1 + \beta^*(p^* - p_0^*)\right], \tag{7}$$

where τ_0^* denotes the yield stress at a reference pressure p_0^* and β^* is the yield-stress growth coefficient. Hermoso *et al.* reported values of the dimensionless piezo-yield coefficient, $\beta_\tau^* = \tau_0^*\beta^*$, at different temperatures from 40 to 140 °C, in the range 1-132 $\times 10^{-4}$ Pa/bars.[28] For the variation of the plastic viscosity, they employed a Barus-type (i.e., exponential) equation. The linear law (7) corresponds to the so-called Drucker-Prager plasticity (flow/no-flow) criterion in solid mechanics, which can be viewed as a simplification of the Mohr-Coulomb plasticity criterion, where τ_0^* is the cohesion and $\tau_0^*\beta^* = \tan(\delta_s)$, δ_s being the internal frictional angle.[24]

In the last few years, a number of studies concerned numerical simulations of flows of viscoplastic materials with pressure-dependent material parameters. Staron *et al.* investigated numerically the discharge of a granular silo, which, for small and moderate outlets, is characterized by a constant discharge rate in contrast with the clepsydra for which the flow velocity depends on the height of the fluid left in the container.[29] Implementing plastic rheology [i.e., $\mu(I)$ rheology], they were able to explain the so-called Beverloo scaling only by means of the pressure dependence of the yield stress. Ionescu *et al.*[24] carried out finite-element simulations of the

granular column collapse problem over inclined planes using the Bingham-plastic constitutive equation and assuming that the yield stress varies linearly with pressure. The plastic viscosity was taken either constant or variable depending on both the pressure and the rate of strain [$\mu(I)$ rheology]. Daviet and Bertails-Descourbes proposed a non-smooth complex optimization numerical framework for the simulation of dense granular flows assuming that the material behaves as a Bingham plastic whose yield stress varies linearly with pressure while the plastic viscosity is constant.[30] They pointed out that this assumption implies that grain-grain interactions mostly involve rigid-body contacts with Coulomb friction. Khouja *et al.* analyzed a regularized Bingham model with pressure-dependent yield stress in the framework of stationary flows and investigated existence, uniqueness, and regularity.[31] They showed that the model can be solved and approximated as far as the frictional parameter is small enough.

Recently, Fusi considered non-isothermal flows of a Bingham plastic with the plastic viscosity and the yield stress depending on both the temperature and pressure.[32] More specifically, he used a perturbation approach to derive the Oberbeck-Boussinesq approximation for a Bingham fluid under the assumption that the Reynolds number is of order one and considered the cases where the Froude number is either small or of order one. Fusi used an exponential expression describing the dependence of the plastic viscosity on the pressure and the temperature and a linear one for the yield stress (such that both rheological parameters increase with pressure and decrease with temperature).[32]

The present work is motivated by the recent work of Fusi *et al.*[33] who presented a novel technique for modeling the lubrication flow of a Bingham plastic in a two-dimensional channel of non-uniform thickness. Under the lubrication approximation, the yield surface and the two velocity components are calculated from the pressure by means of closed form expressions while the pressure satisfies an integro-differential equation. This was solved by Fusi *et al.* with an iterative procedure.[33] Fusi *et al.* also considered briefly the case of pressure-dependent plastic viscosity and provided some approximations for the case of a slowly varying linear wall.[33]

The advantage of the method of Fusi *et al.*[33] is that the lubrication paradox is avoided and the correct shape of the yield surface which is opposite to that of the wall is approximated at zero order. With other approaches, the correct shape of the yield surface is obtained after calculating higher-order solutions.[34,35] In asymptotic analyses where the pressure gradient is obtained from the constraint of a unit areal flux in the x-direction at the leading order, the yield surface variation (at zero order) is similar to that of the wall due to the scaling with the mean velocity. The lubrication paradox arises from the fact that the predicted plug is not a true unyielded region since the leading order velocity varies in the x-direction. Thus, the position of the yield surface needs to be corrected by calculating higher-order solutions.[34,35]

Nevertheless, since the pressure is scaled with the pressure difference between inlet and outlet planes of the channel and the stress components with the pressure difference times the (small) aspect ratio of the channel, a prerequisite of the model of Fusi *et al.* is that the unyielded region (plug) extends from the inlet to the outlet plane as well.[33] Therefore, the model cannot be applied when the plug is broken. Consequently, the results of Ref. 33 in this latter case are not reliable. For example, the calculated transverse velocity contours cross the symmetry plane where this velocity component should vanish.

The objectives of the present work are (a) the extension of the method of Fusi *et al.*[33] for solving the lubrication flow of a Herschel-Bulkley fluid with pressure-dependent consistency index and yield stress in a symmetric channel of non-constant width; (b) the derivation of analytical solutions for certain limiting cases, such as the flows in a channel of constant or linearly varying width; and (c) the investigation of the advantages and the limitations of the method.

Fusi *et al.* derived solutions of plane Poiseuille and Couette flows of a Bingham plastic and determined conditions for existence or non-existence of a rigid plug under the assumption that the velocity is one-dimensional while the pressure in the yielded region is two-dimensional.[36] They derived explicit solutions for the case where the yield stress follows the linear equation (7) and the plastic viscosity also varies linearly and vanishes at zero relative pressure, i.e.,

$$\mu^*(p^*) = \overline{\alpha}^*(p^* - p_0^*), \tag{8}$$

where the constant $\bar{\alpha}^*$ has time units. With the latter assumption, the derivation of an analytical solution becomes easier, but the flows of a Bingham plastic with constant rheological parameters or with constant plastic viscosity are not special cases of the flow considered. This shortcoming was avoided by Damianou and Georgiou[37] who analyzed the same flow using

$$\mu^*(p^*) = \mu_0^*\left[1 + \alpha^*(p^* - p_0^*)\right] \tag{9}$$

instead. In the present work, with the use of the lubrication method of Fusi *et al.*,[33] the study of viscoplastic Poiseuille flows with a general wall function and pressure-dependent rheological parameters is possible.

In Sec. II, the lubrication equations are presented for the general case of a Herschel-Bulkley fluid with the consistency index and the yield stress being (general) functions of pressure. The zero-order solution is derived semi-analytically, in the sense that closed-form expressions are derived for the two velocity components in terms of the pressure, which is found by solving an integro-differential equation numerically. As mentioned earlier, the solutions hold as long as the unyielded core extends continuously from the inlet to the outlet plane. Compared to Ref. 33, the presentation of the method is considerably simpler despite considering a more general flow problem. In Sec. III, we derive analytical solutions for the case of a channel of constant width with special forms, i.e., linear and exponential, of the consistency-index and yield-stress pressure-dependence functions. The yield-stress growth parameter is allowed to be negative, and the applicability windows of the method in terms of the various parameters are determined. In Sec. IV, channels of linearly varying width (converging and diverging channels) are considered and semi-analytical solutions are derived for the case of a Bingham plastic with both the yield stress and the plastic viscosity varying linearly with pressure. The applicability and the limitations of the method are again discussed. In Sec. V, we present

numerical results for more complex geometries. In contrast to the work of Fusi *et al.*,[33] the integro-differential equation for the pressure is solved directly (not iteratively) by means of a standard pseudo-spectral numerical method. Finally, in Sec. VI, the conclusions are summarized and future research plans are discussed.

II. DERIVATION OF THE MODEL

We consider a Herschel-Bulkley fluid, i.e., a fluid obeying constitutive equation (3), where however the consistency index k^* and the yield stress τ_y^* are pressure dependent. For the sake of generality, we assume that

$$k^*(p^*) = k_0^* f(\alpha^*(p^* - p_0^*)) \tag{10}$$

and

$$\tau_y^*(p^*) = \tau_0^* g(\beta^*(p^* - p_0^*)), \tag{11}$$

where k_0^* is the consistency index at the reference pressure (assumed to be the same for the two material parameters) and f and g are appropriate increasing functions such that $f(0) = g(0) = 1$. For example, in Eqs. (4) and (5), we have $f(x) = e^x$ and $f(x) = 1 + x$, respectively, and in Eq. (7) $g(x) = 1 + x$.

Assume now the pressure-driven flow of an incompressible Herschel-Bulkley fluid in a symmetric long channel of length L^* and variable width $2h^*(x^*)$, as illustrated in Fig. 1, where only the upper part of the domain is shown due to symmetry. A pressure p_{in}^* is applied at the inlet of the channel ($x^* = 0$) while the pressure at the exit ($x^* = L^*$) is $p_{out}^* < p_{in}^*$, i.e., the imposed pressure difference is $\Delta p^* = p_{in}^* - p_{out}^*$. The main flow is in the x^* direction, and the z^*-velocity component is zero. Hence, the velocity vector is of the form $\mathbf{v}^* = v_x^*(x^*, y^*)\mathbf{i} + v_y^*(x^*, y^*)\mathbf{j}$. In the flow of interest (Fig. 1), the

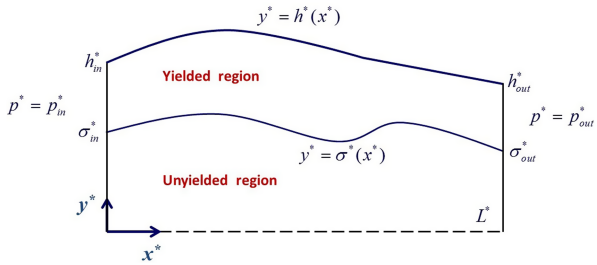

FIG. 1. Geometry, some definitions, and boundary conditions for the dimensional flow in a symmetric channel of length L^* and variable width $2h^*(x^*)$ with an unyielded core of width $\sigma^*(x^*)$. Due to symmetry, only half of the flow domain is shown.

yielded and the unyielded regions are separated by the interface $y^* = \sigma^*(x^*)$ for $0 \le x^* \le L^*$, where $0 < \sigma^*(x^*) < h^*(x^*)$. Hence, the unyielded region extends from the inlet to the outlet plane, i.e., the plug is not broken. Moreover, if $\sigma^*(x^*) = h^*(x^*)$ at any point x^*, the unyielded region touches the wall, and due to the no-slip boundary condition, there is no flow. Let also $\sigma_{in}^* \equiv \sigma^*(0)$ and $\sigma_{out}^* \equiv \sigma^*(L^*)$.

In the yielded region, the continuity equation and the x- and y-components of the momentum equation are simplified as follows:

$$\frac{\partial v_x^*}{\partial x^*} + \frac{\partial v_y^*}{\partial y^*} = 0, \tag{12}$$

$$\rho^*\left(v_x^*\frac{\partial v_x^*}{\partial x^*} + v_y^*\frac{\partial v_x^*}{\partial y^*}\right) = -\frac{\partial p^*}{\partial x^*} + \frac{\partial \tau_{xx}^*}{\partial x^*} + \frac{\partial \tau_{yx}^*}{\partial y^*}, \tag{13}$$

$$\rho^*\left(v_x^*\frac{\partial v_y^*}{\partial x^*} + v_y^*\frac{\partial v_y^*}{\partial y^*}\right) = -\frac{\partial p^*}{\partial y^*} + \frac{\partial \tau_{xy}^*}{\partial x^*} + \frac{\partial \tau_{yy}^*}{\partial y^*}, \tag{14}$$

where ρ^* is the density. The non-zero components of the stress tensor in the yielded regime read

$$\left.\begin{aligned}
\tau_{xx}^* &= 2\left\{\frac{\tau_0^* g(\beta^*(p^* - p_0^*))}{\dot\gamma^*} + k_0^* f(a^*(p^* - p_0^*))\dot\gamma^{*n-1}\right\}\frac{\partial v_x^*}{\partial x^*}\\
\tau_{yx}^* &= \left\{\frac{\tau_0^* g(\beta^*(p^* - p_0^*))}{\dot\gamma^*} + k_0^* f(a^*(p^* - p_0^*))\dot\gamma^{*n-1}\right\}\left(\frac{\partial v_x^*}{\partial y^*} + \frac{\partial v_y^*}{\partial x^*}\right)\\
\tau_{yy}^* &= 2\left\{\frac{\tau_0^* g(\beta^*(p^* - p_0^*))}{\dot\gamma^*} + k_0^* f(a^*(p^* - p_0^*))\dot\gamma^{*n-1}\right\}\frac{\partial v_y^*}{\partial y^*}
\end{aligned}\right\}, \quad \sigma^*(x^*) \le y^* \le h^*(x^*), \tag{15}$$

where

$$\dot\gamma^* = \sqrt{4\left(\frac{\partial v_x^*}{\partial x^*}\right)^2 + \left(\frac{\partial v_x^*}{\partial y^*} + \frac{\partial v_y^*}{\partial x^*}\right)^2} \tag{16}$$

(note that the continuity equation has been used). Similarly, the magnitude of the stress tensor is given by

$$\tau^* = \sqrt{\frac{1}{2}\mathrm{tr}\boldsymbol{\tau}^{*2}} = \sqrt{\frac{1}{2}\tau_{xx}^{*2} + \frac{1}{2}\tau_{yy}^{*2} + \tau_{yx}^{*2}}. \tag{17}$$

Without loss of generality, we assume here that the reference pressure that appears in Eqs. (10) and (11) is $p_0^* = p_{out}^*$.

The unyielded core, defined by $\Omega^* = \{(x^*, y^*): x^* \in [0, L^*], y^* \in [0, \sigma^*]\}$, moves in the x-direction as a solid, i.e., at constant velocity v_c^*. Thus,

$$v_x^* = v_c^* \quad \text{and} \quad v_y^* = 0 \quad \text{for} \quad 0 \le y^* \le \sigma^*(x^*). \tag{18}$$

For a steady-state flow in the absence of body forces, the integral balance of linear momentum of the whole plug core yields the following equation:[33]

$$\int_0^{L^*} \left[-\sigma_x^*(-p^* + \tau_{xx}^*) + \tau_{yx}^*\right]_{y^*=\sigma^*} dx^* + p_{in}^*\sigma_{in}^* - p_{out}^*\sigma_{out}^* = 0, \tag{19}$$

where $\sigma_x^* \equiv d\sigma^*/dx^*$. Equation (19) simply implies that τ_{yx}^* acts on dx^* and $-p^* + \tau_{xx}^*$ acts on $dy^* = \sigma_x^* dx^*$, where dx^* and

dy^* define an infinitesimal element of the longitudinal side of the core.

A. Non-dimensional formulation

We assume that the length L^* of the channel is much greater than its greatest semi-width, i.e., $L^* \gg H^* \equiv \max_{x\in[0,L^*]} h^*(x^*)$, and introduce the dimensionless parameter

$$\varepsilon \equiv \frac{H^*}{L^*} \ll 1, \tag{20}$$

which is used for applying the classical lubrication approximation or thin-film approach.[34] The problem is dedimensionalised by scaling x^* by L^*, y^*, h^*, and σ^* by H^*, $(p^* - p^*_{out})$ by Δp^*, v_x^* by $H^*(\varepsilon\Delta p^*/k_0^*)^{1/n}$, v_y^* by $\varepsilon H^*(\varepsilon\Delta p^*/k_0^*)^{1/n}$, and the stress components by $\varepsilon\Delta p^*$. The dimensionless forms of the continuity equation and the two components of the momentum equation are as follows:

$$\frac{\partial v_x}{\partial x} + \frac{\partial v_y}{\partial y} = 0, \tag{21}$$

$$\varepsilon^{2/n-1} Re\left(v_x\frac{\partial v_x}{\partial x} + v_y\frac{\partial v_x}{\partial y}\right) = -\frac{\partial p}{\partial x} + \varepsilon\frac{\partial \tau_{xx}}{\partial x} + \frac{\partial \tau_{yx}}{\partial y}, \tag{22}$$

$$\varepsilon^{2/n+1} Re\left(v_x\frac{\partial v_y}{\partial x} + v_y\frac{\partial v_y}{\partial y}\right) = -\frac{\partial p}{\partial y} + \varepsilon^2\frac{\partial \tau_{yx}}{\partial x} + \varepsilon\frac{\partial \tau_{yy}}{\partial y}, \tag{23}$$

where Re is the Reynolds number defined by

$$Re \equiv \frac{\rho^* H^{*3}\Delta p^{*2/n-1}}{k_0^{*2/n} L^*}. \tag{24}$$

Note that for $n = 1$, the equations for the Bingham case are recovered, in agreement with the analysis of Fusi *et al.*[33] For the stress components, one gets

$$\left.\begin{aligned}
\tau_{xx} &= 2\varepsilon\left[\frac{Bn\, g(\beta p)}{\dot\gamma} + f(\alpha p)\dot\gamma^{n-1}\right]\frac{\partial v_x}{\partial x}\\
\tau_{yx} &= \left[\frac{Bn\, g(\beta p)}{\dot\gamma} + f(\alpha p)\dot\gamma^{n-1}\right]\left(\frac{\partial v_x}{\partial y} + \varepsilon^2\frac{\partial v_y}{\partial x}\right)\\
\tau_{yy} &= 2\varepsilon\left[\frac{Bn\, g(\beta p)}{\dot\gamma} + f(\alpha p)\dot\gamma^{n-1}\right]\frac{\partial v_y}{\partial y}
\end{aligned}\right\}, \quad \sigma(x) \le y \le h(x), \tag{25}$$

where

$$\dot\gamma = \sqrt{4\varepsilon^2\left(\frac{\partial v_x}{\partial x}\right)^2 + \left(\frac{\partial v_x}{\partial y} + \varepsilon^2\frac{\partial v_y}{\partial x}\right)^2}. \tag{26}$$

In Eq. (25), there appear three dimensionless numbers, the Bingham number Bn and the consistency-index and yield-stress growth numbers a and β, which are defined by

$$Bn \equiv \frac{\tau_0^*}{\varepsilon\,\Delta p^*}, \quad \alpha \equiv a^*\Delta p^*, \quad \beta \equiv \beta^*\Delta p^*. \tag{27}$$

It is clear that when $\beta \ge 0$ the dimensionless yield stress is reduced from $g(\beta)Bn$ at the inlet plane to Bn at the exit plane. When $\beta < 0$, then the dimensionless yield stress increases from $g(\beta)Bn$ to Bn. We thus have the constraint $g(\beta) > 0$ so that the unyielded core extends from the inlet to the outlet plane (otherwise the present model is not valid).

Finally, the dimensionless form of Eq. (19) is

$$\int_0^1 \left[-\sigma_x(-p + \varepsilon\tau_{xx}) + \tau_{yx}\right]_{y=\sigma} dx + \sigma_{in} = 0, \tag{28}$$

where the dimensionless pressure satisfies the following boundary conditions:

$$p(0, \sigma_{in}) = 1, \quad p(1, \sigma_{out}) = 0. \tag{29}$$

B. The zero-order problem

Following Fusi *et al.*,[33] we solve the zero-order problem. For the sake of simplicity, we will avoid introducing new symbols for the zero-order variables; hence, hereafter all variables are the zero-order ones. The continuity and momentum equations at zero order read as follows:

$$\frac{\partial v_x}{\partial x} + \frac{\partial v_y}{\partial y} = 0, \tag{30}$$

$$-\frac{\partial p}{\partial x} + \frac{\partial \tau_{yx}}{\partial y} = 0, \tag{31}$$

$$-\frac{\partial p}{\partial y} = 0. \tag{32}$$

From the last equation, it is deduced that $p = p(x)$. At zero order, $\tau_{xx} = \tau_{yy} = 0$ while

$$\tau_{yx} = \left[\frac{Bn\, g(\beta p)}{\dot\gamma} + f(\alpha p)\dot\gamma^{n-1}\right]\frac{\partial v_x}{\partial y}, \quad \sigma(x) \le y \le h(x). \tag{33}$$

Working in the upper part of the channel, we note that in the yielded region $\dot\gamma = |\partial v_x/\partial y| = -\partial v_x/\partial y$ and thus

$$\tau_{yx} = -Bn\, g(\beta p) - f(\alpha p)\left(-\frac{\partial v_x}{\partial y}\right)^n, \quad \sigma(x) \le y \le h(x). \tag{34}$$

Substituting the above expression into the x-momentum equation (31), integrating twice, and applying the boundary conditions $\partial v_x/\partial y(x, \sigma) = v_x(x, h) = 0$, the following expression is obtained for v_x:

$$v_x(x, y) = \left[1 - \frac{(y-\sigma)^{1+1/n}}{(h-\sigma)^{1+1/n}}\right]v_c, \quad \sigma(x) \le y \le h(x), \tag{35}$$

where

$$v_c = \frac{(-p_x)^{1/n}(h-\sigma)^{1+1/n}}{(1+1/n)f^{1/n}(\alpha p)} \tag{36}$$

is the velocity of the unyielded core and $p_x \equiv dp/dx$. The fact that the RHS of the above equation is constant will be utilised below in order to derive the integro-differential equation governing the pressure.

The transverse velocity component is found from the continuity equation (30). Given that $v_y(x, h) = 0$, we can write

$$v_y = \int_y^h \frac{\partial v_x}{\partial x}\, dy. \tag{37}$$

Substituting v_x from Eq. (35) and carrying out the required differentiation and integration, one gets

$$v_y = \frac{v_c}{2+1/n}\left[\sigma_x + (1+1/n)h_x - (2+1/n)\left(\frac{y-\sigma}{h-\sigma}\right)^{1+1/n}\sigma_x - (1+1/n)(h_x-\sigma_x)\left(\frac{y-\sigma}{h-\sigma}\right)^{2+1/n}\right], \tag{38}$$

where $h_x \equiv dh/dx$. The satisfaction of condition $v_y(x, \sigma) = 0$ requires that

$$\sigma_x + (1+1/n)h_x = 0. \tag{39}$$

Equation (38) can then be simplified to

$$v_y = (1+1/n)v_c \frac{(y-\sigma)^{1+1/n}}{(h-\sigma)^{2+1/n}}(h-y)\,h_x. \tag{40}$$

From Eq. (39), it is deduced that the semi-width of the unyielded core is given by

$$\sigma(x) = -(1+1/n)h(x) + C, \tag{41}$$

where C is an unknown constant to be determined. The above result generalizes the result of Fusi *et al.*[33] for a Bingham plastic ($n = 1$). Equation (41) implies that the width of the unyielded core increases when the wall function $h(x)$ is decreasing and vice versa. The rate of change of σ is $(1 + 1/n)$ times the rate of change of h and is independent of the other material and flow parameters, which affect only the constant C. Hence, decreasing the power-law exponent n in a converging channel causes the plug to expand faster, which is expected, given that the velocity profile becomes flatter as shear thinning is enhanced. To determine the constant C, we return to the plug momentum balance equation (28), which at zero order becomes

$$\int_0^1 \left[\sigma_x p + \tau_{yx}\right]_{y=\sigma} dx + \sigma_{in} = 0. \tag{42}$$

Since at the rigid core surface ($y = \sigma$) the rate of strain vanishes, $\partial v_x/\partial y = 0$, Eq. (34) gives

$$\tau_{yx}\Big|_{y=\sigma} = -Bn\, g(\beta p). \tag{43}$$

Therefore

$$\int_0^1 \left[\sigma_x p - Bn\, g(\beta p)\right] dx + \sigma_{in} = 0. \tag{44}$$

Using integration by parts and Eq. (41), we find that

$$C = Bn\int_0^1 g(\beta p)dx - (1+1/n)\int_0^1 p_x h dx = Bn\int_0^1 g(\beta p)dx + (1+1/n)\left[h_{in} + \int_0^1 p h_x dx\right]. \tag{45}$$

From Eq. (36), we observe that

$$\frac{d}{dx}\left[\frac{p_x}{f(\alpha p)}(h-\sigma)^{n+1}\right] = 0, \tag{46}$$

which gives

$$p_{xx} - \frac{\alpha f'(\alpha p)p_x^2}{f(\alpha p)} + \frac{p_x}{h-\sigma}(n+1)(h_x - \sigma_x) = 0. \tag{47}$$

By means of Eqs. (39) and (45), we get the following integro-differential equation for the pressure:

$$p_{xx} + \left[\frac{(n+1)(2+1/n)h_x}{(2+1/n)h - Bn\int_0^1 g(\beta p)dx + (1+1/n)\int_0^1 p_x h dx} - \frac{\alpha f'(\alpha p)p_x}{f(\alpha p)}\right]p_x = 0 \tag{48}$$

subject to the boundary conditions $p(0) = 1$ and $p(1) = 0$. An alternative form of Eq. (48) is

$$p_{xx} + \left[\frac{(n+1)(2+1/n)h_x}{(2+1/n)h - (1+1/n)h_{in} - Bn\int_0^1 g(\beta p)dx - (1+1/n)\int_0^1 p h_x dx} - \frac{\alpha f'(\alpha p)p_x}{f(\alpha p)}\right]p_x = 0. \tag{49}$$

Once the pressure $p(x)$ is known, the yield surface, the unyielded core velocity, and the two velocity components are readily calculated by means of Eqs. (41), (36), (35), and (40), respectively. For the volumetric flow rate (which is, of course, constant along the channel), we have

$$Q = 2\left(\int_0^\sigma v_c dy + \int_\sigma^h v_x dy\right) = \frac{2v_c}{2+1/n}[\sigma + (1+1/n)h] = \frac{2v_c C}{2+1/n}. \tag{50}$$

Equation (49) can be solved numerically, using, for example, finite element or pseudo-spectral methods. Analytical solutions are possible only for channels of constant or linearly varying width when functions f and g are of simple form. These are presented and discussed in Secs. III and IV.

III. FLOW IN A CHANNEL OF CONSTANT WIDTH

In the case of a channel of constant width, $h = 1$ and $h_x = 0$; thus, Eq. (49) is simplified to

$$p_{xx} - \frac{\alpha f'(\alpha p)}{f(\alpha p)} p_x^2 = 0, \tag{51}$$

which implies that the pressure distribution is independent of the yield-stress function and the power-law exponent. The former affects only the location of the yield point, which is constant along the channel since Eqs. (41) and (45) give

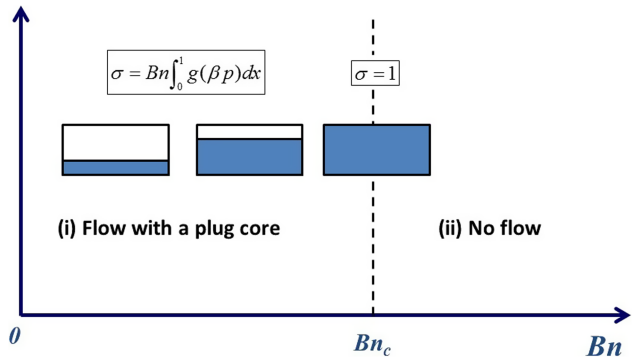

FIG. 2. Flow regimes as the Bingham number is increased in the lubrication flow of a viscoplastic fluid in a channel of constant width. When $Bn < Bn_c$, an unyielded region of constant height is predicted even when the yield stress and the consistency index are pressure-dependent. Note that $Bn \equiv \tau_0^*/(\varepsilon \Delta p^*)$.

$$\sigma = Bn \int_0^1 g(\beta p)dx. \tag{52}$$

Moreover, the transverse velocity component vanishes, $v_y = 0$, while $v_x = v_x(y)$.

It is clear that when $\sigma = 1$, there is no flow since the unyielded core touches the wall at which no-slip applies. There are thus two flow regimes depending on the value of the Bingham number, as illustrated in Fig. 2. The critical Bingham number at which there is no flow,

$$Bn_c = \frac{1}{\int_0^1 g(\beta p)dx} \tag{53}$$

is obviously inversely proportional to the lowest dimensional pressure difference above which yielding occurs ($\Delta p_c^* = \tau_0^*/(\varepsilon Bn_c)$).

From Eq. (51), we observe that

$$\frac{p_x}{f(\alpha p)} = -K, \tag{54}$$

where K is a constant that can be determined along with the pressure p upon integration and application of the two boundary conditions for p. It is easily found that

$$v_c = \frac{K^{1/n}(1-\sigma)^{1+1/n}}{(1+1/n)} \tag{55}$$

and

$$v_x(y) = \left[1 - \frac{(y-\sigma)^{1+1/n}}{(1-\sigma)^{1+1/n}}\right] v_c, \quad \sigma \le y \le 1. \tag{56}$$

Table I tabulates expressions of K, $p(x)$, and σ for the cases where f and g are linear and/or exponential. Note that these results are independent of the power-law exponent n, which affects only the velocity profile (56).

TABLE I. Expressions for the constant K, the pressure $p(x)$, and the yield point σ for different functions describing the pressure-dependence of the consistency index ($f(x)$) and the yield stress ($g(x)$) in the case of a channel of constant width. These are independent of the power-law exponent n.

$f(x)$	K	$p(x)$	$g(x)$	$\frac{\sigma}{Bn} = \int_0^1 g(\beta p)dx$
1	1	$1-x$	1	1
			$1+x$	$1+\frac{\beta}{2}$
			e^x	$\frac{e^\beta - 1}{\beta}$
$1+x$	$\frac{\ln(1+\alpha)}{\alpha}$	$\frac{1}{\alpha}\left[(1+\alpha)^{1-x} - 1\right]$	1	1
			$1+x$	$1+\left[\frac{1}{\ln(1+\alpha)} - \frac{1}{\alpha}\right]\beta$
			e^x	$e^{-\beta/a}\int_0^1 e^{\frac{\beta}{a}(1+\alpha)^{1-x}}dx$
e^x	$\frac{1-e^{-\alpha}}{\alpha}$	$\frac{1}{\alpha}\ln\frac{1}{(1-e^{-\alpha})x + e^{-\alpha}}$	1	1
			$1+x$	$\frac{\beta\left[1-(1+\alpha)e^{-\alpha}\right]}{\alpha(1-e^{-\alpha})}$
			e^x	$\frac{\alpha}{1-e^{-a}}, \quad \beta = \alpha$
				$\frac{\alpha(1-e^{\beta-a})}{(\alpha-\beta)(1-e^{-a})}, \quad \beta \neq \alpha$

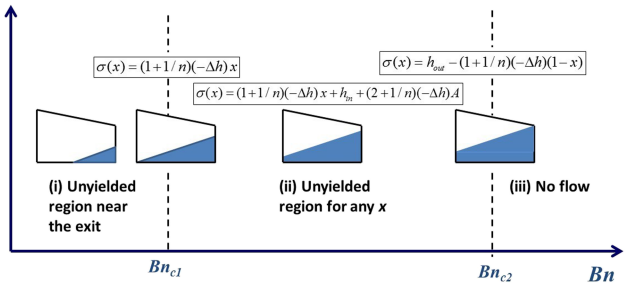

FIG. 3. Flow regimes for the Herschel-Bulkley flow in the case of a linearly converging channel. The present lubrication analysis holds only in regime (ii).

Below we discuss the case where both the consistency index and the yield stress vary linearly with pressure, i.e., $f(x) = g(x) = 1 + x$. From Table I, we see that when $\alpha > 0$

$$p(x) = \frac{1}{a}\left[(1+\alpha)^{1-x} - 1\right] \tag{57}$$

and

$$\sigma = \left\{1 + \left[\frac{1}{\ln(\alpha+1)} - \frac{1}{\alpha}\right]\beta\right\} Bn. \tag{58}$$

Flow occurs provided that the Bingham number is lower than the critical value,

$$Bn_c \equiv \frac{1}{1 + \left[\frac{1}{\ln(\alpha+1)} - \frac{1}{\alpha}\right]\beta}. \tag{59}$$

(Recall that the above number is inversely proportional to the lowest dimensional pressure difference above which yielding occurs.) Note that β may be negative in which case the yield stress is increasing downstream and thus Bn_c may be greater than unity. If $\beta = 0$, then $Bn_c = 1$ and $\sigma = Bn$, i.e., σ is independent of the consistency-index growth parameter α (this is due to the fact that the pressure is scaled by the inlet pressure Δp^*). As discussed below, this is also the case when solving the standard Poiseuille flow problem without the lubrication approximation. The present lubrication model is valid provided that $\sigma \geq 0$, i.e.,

$$\beta \geq \frac{\alpha \ln(\alpha+1)}{\ln(\alpha+1) - \alpha} \tag{60}$$

so that the plug is not broken. As already mentioned, β may be negative and, more specifically, $\beta \geq -1$ (so that the yield stress in the channel remains positive), which ensures that condition (60) is satisfied (the left hand side is always less than −2).

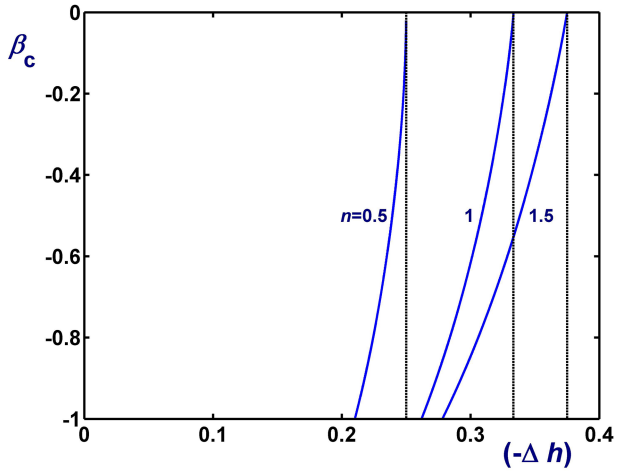

FIG. 4. Lower bounds of the yield-stress growth parameter for the flow of a Herschel-Bulkley fluid with constant consistency index ($\alpha = 0$) and yield stress varying linearly with pressure in a converging channel with $h(x) = 1 + \Delta h\, x$ for various values of the power-law exponent. As $(-\Delta h)$ is increased from 0 (flat channel) to the critical value of $1/(2 + 1/n)$ (corresponding to no flow and indicated by the vertical line in each case), the lower admissible value of β is initially −1 and then increases rapidly to 0.

For a Bingham plastic ($n = 1$), the velocity is given by

$$v_x = \begin{cases} \frac{\ln(\alpha+1)}{2\alpha}(1-y)(1+y-2\sigma), & \sigma \leq y \leq 1 \\ \frac{\ln(\alpha+1)}{2\alpha}(1-\sigma)^2, & 0 \leq y \leq \sigma \end{cases}, \tag{61}$$

where the effects of Bn and β are accounted for via the yield point σ.

When the plastic viscosity is pressure-independent ($\alpha = 0$), we find the standard linear pressure distribution for the Poiseuille flow

$$p(x) = 1 - x, \tag{62}$$

where, however, the yield point depends on the yield-stress growth number,

$$\sigma = (1 + \beta/2)\, Bn. \tag{63}$$

For the velocity, we now have

$$v_x = \begin{cases} \frac{1}{2}(1-y)(1+y-2\sigma), & \sigma \leq y \leq 1 \\ \frac{1}{2}(1-\sigma)^2, & 0 \leq y \leq \sigma \end{cases} \tag{64}$$

and the critical Bingham number above which there is no flow is

$$Bn_c \equiv \frac{1}{1 + \beta/2}. \tag{65}$$

(Recall that $\beta \geq -1$.)

For the case of a Bingham plastic ($n = 1$) with linearly varying yield stress and plastic viscosity ($g(x) = f(x) = 1 + x$), the analytical Poiseuille flow solution can be obtained,[37]

$$p(x,y) = \begin{cases} \frac{1}{\alpha}\left[(1+\alpha)^{1-x}\frac{\cosh\left[\varepsilon\,\ln(1+\alpha)(y-\sigma) + \tanh^{-1}(\varepsilon Bn\beta)\right]}{\cosh\left[\tanh^{-1}(\varepsilon Bn\beta)\right]} - 1\right], & \sigma \leq y \leq 1 \\ \frac{1}{\alpha}\left[(1+\alpha)^{1-x} - 1\right], & 0 \leq y < \sigma \end{cases}. \tag{66}$$

As for the velocity, one finds

$$v_x(y) = \begin{cases} \dfrac{1}{\alpha\varepsilon^2 \ln(1+\alpha)} \ln \dfrac{\cosh\left[\varepsilon \ln(1+\alpha)(1-\sigma) + \tanh^{-1}(\varepsilon Bn\beta)\right]}{\cosh\left[\varepsilon \ln(1+\alpha)(y-\sigma) + \tanh^{-1}(\varepsilon Bn\beta)\right]} - \dfrac{Bn\beta}{\alpha}(1-y), & \sigma \le y \le 1 \\ \dfrac{1}{\alpha\varepsilon^2 \ln(1+\alpha)} \ln \dfrac{\cosh\left[\varepsilon \ln(1+\alpha)(1-\sigma) + \tanh^{-1}(\varepsilon Bn\beta)\right]}{\cosh\left[\tanh^{-1}(\varepsilon Bn\beta)\right]} - \dfrac{Bn\beta}{\alpha}(1-\sigma), & 0 \le y < \sigma \end{cases}, \tag{67}$$

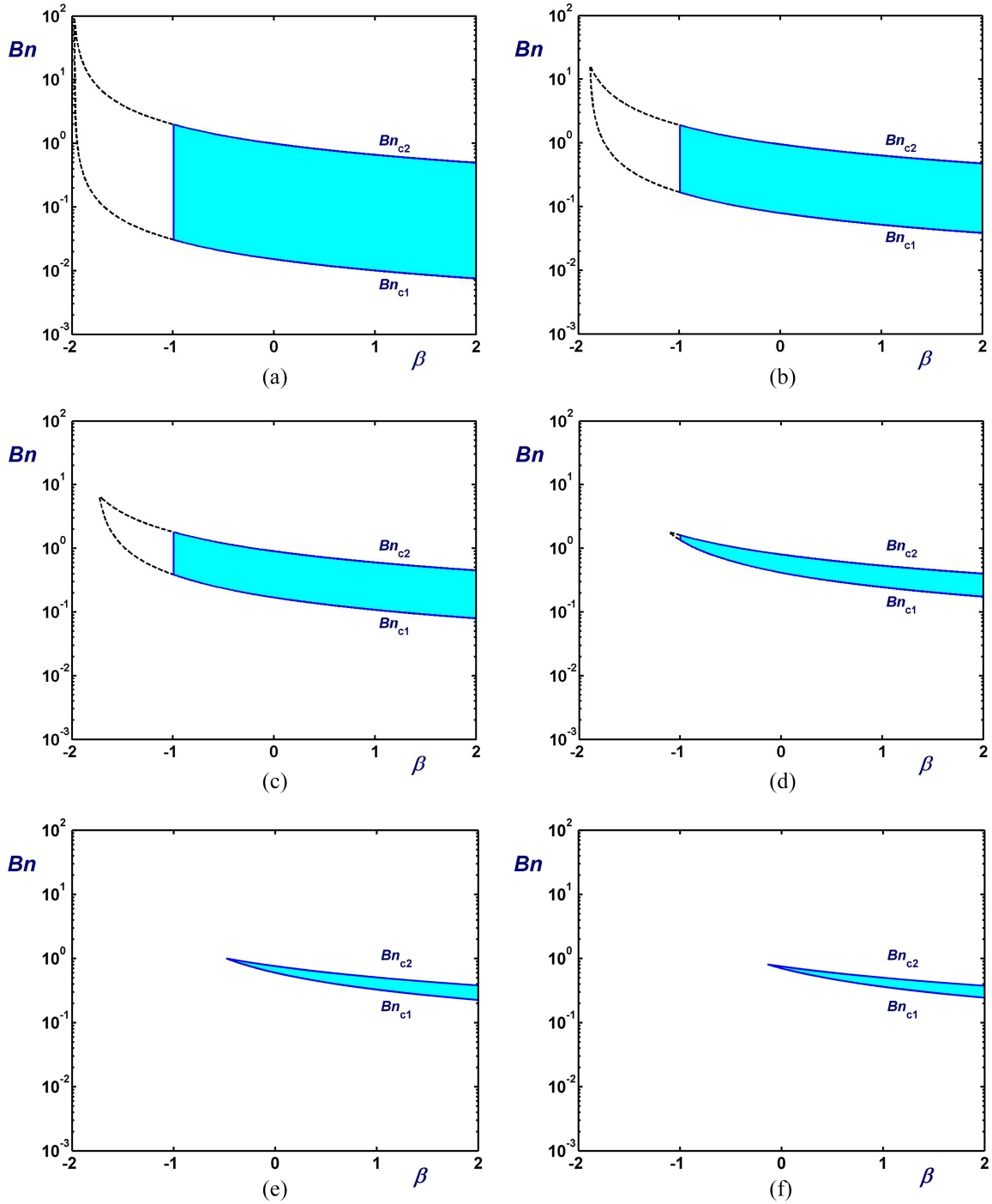

FIG. 5. Critical Bingham numbers in the case of Herschel-Bulkley flow with $n = 0.5$ in a linearly converging channel ($h_{in} = 1$) with constant consistency index ($\alpha = 0$) and linearly varying yield stress: (a) $\Delta h = -0.01$; (b) $\Delta h = -0.05$; (c) $\Delta h = -0.1$; (d) $\Delta h = -0.2$; (e) $\Delta h = -0.24$; (f) $\Delta h = -0.249$. The shaded region is the applicability domain of the present method. As $(-\Delta h)$ is increased from 0 (flat channel) to the critical value of 0.25 (no flow), the lower admissible value of β increases from −1 to 0.

where σ is given by Eq. (58), i.e., it is the same as that predicted by the lubrication approximation. The main difference between the above analytical solutions from the lubrication one is that the pressure in the yielded domain is two dimensional. The pressure in the unyielded core is identical to the pressure predicted by the lubrication approximation for both yielded and unyielded regions. Setting $\sigma = Bn = 0$ yields the solution of a Newtonian fluid with a pressure-dependent viscosity,[12] and taking only the first term of the Taylor expansion of Eq. (67) in terms of ε yields the lubrication solution (61). The effects of the various parameters on the yield point σ, as discussed in Ref. 37, apply here (see also a recent solution of the axisymmetric flow in Ref. 38). With the lubrication assumption, the velocity profile is slightly overestimated and the relative differences are enhanced as α assumes rather high values.[37]

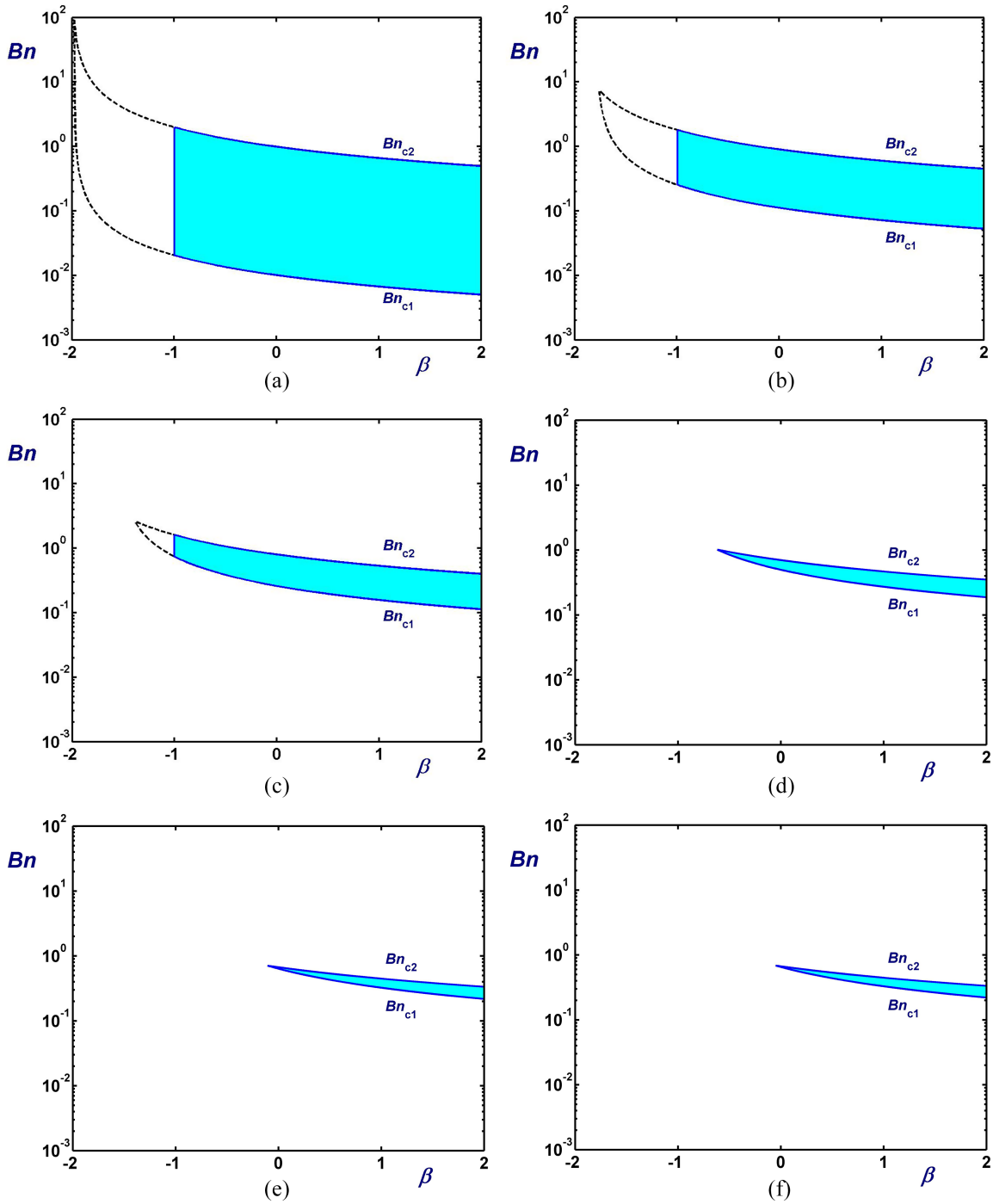

FIG. 6. Critical Bingham numbers in the case of Bingham-plastic flow ($n = 1$) in a linearly converging channel ($h_{in} = 1$) with constant plastic viscosity ($\alpha = 0$) and linearly varying yield stress: (a) $\Delta h = -0.01$; (b) $\Delta h = -0.1$; (c) $\Delta h = -0.2$; (d) $\Delta h = -0.3$; (e) $\Delta h = -0.33$; (f) $\Delta h = -0.332$. The shaded region is the applicability domain of the present method. As $(-\Delta h)$ is increased from 0 (flat channel) to the critical value of 1/3 (no flow), the lower admissible value of β increases from −1 to 0.

IV. FLOW IN A CHANNEL OF LINEARLY VARYING WIDTH

In this section, we consider a channel of linearly varying width such that

$$h(x) = h_{in} + (h_{out} - h_{in})x = h_{in} + \Delta h x \quad \text{and} \quad h_x(x) = \Delta h. \tag{68}$$

From Eq. (41), we know that the yield surface also varies linearly,

$$\sigma(x) = -(1 + 1/n)\Delta h x - (1 + 1/n)h_{in} + C, \tag{69}$$

where by means of Eq. (45), the constant C is given by

$$C = Bn \int_0^1 g(\beta p)dx + (1 + 1/n)h_{in} + (1 + 1/n)\Delta h \int_0^1 p dx. \tag{70}$$

In this case, Eq. (49) can be written as follows:

$$p_{xx} + \left[\frac{n+1}{x+A} - \frac{\alpha f'(\alpha p)p_x}{f(\alpha p)}\right] p_x = 0, \tag{71}$$

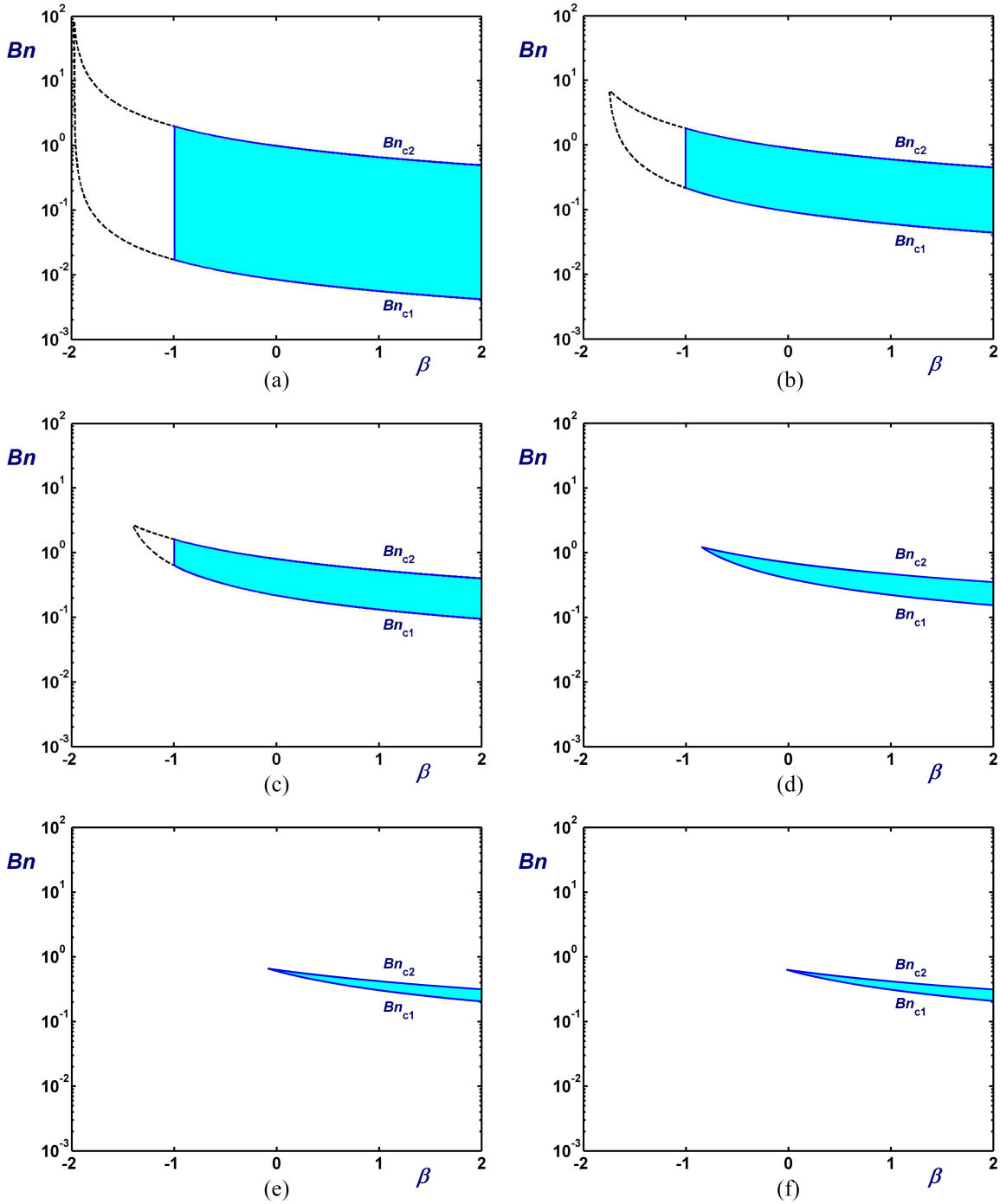

FIG. 7. Critical Bingham numbers in the case of the Herschel-Bulkley flow with $n = 1.5$ in a linearly converging channel ($h_{in} = 1$) with constant consistency index ($\alpha = 0$) and linearly varying yield stress: (a) $\Delta h = -0.01$; (b) $\Delta h = -0.1$; (c) $\Delta h = -0.2$; (d) $\Delta h = -0.3$; (e) $\Delta h = -0.37$; (f) $\Delta h = -0.374$. The shaded region is the applicability domain of the present method. As $(-\Delta h)$ is increased from 0 (flat channel) to the critical value of 3/8 (no flow), the lower admissible value of β increases from −1 to 0.

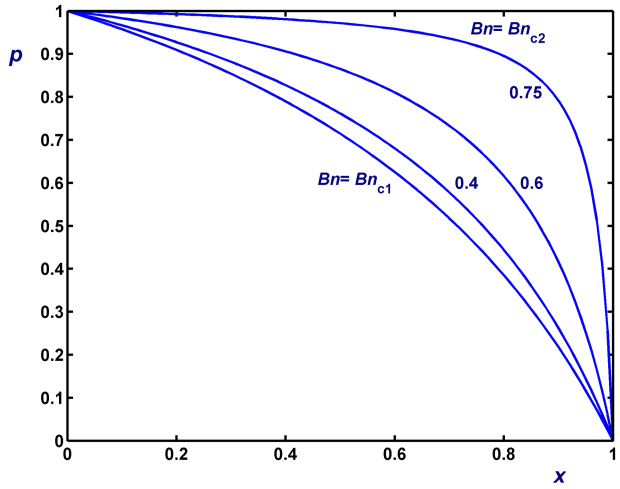

FIG. 8. Pressure distributions in the case of the flow of a Bingham plastic ($n = 1$) with constant rheological parameters ($\alpha = \beta = 0$) in a linearly converging channel with $h(x) = 1 - 0.2x$ for various values of the Bingham number ranging from $Bn_{c1} = 0.2594$ to $Bn_{c2} = 0.8$.

where

$$A = \frac{h_{in} - Bn\int_0^1 g(\beta p)dx - (1 + 1/n)\Delta h\int_0^1 pdx}{(2 + 1/n)\Delta h}. \quad (72)$$

Once A is calculated, the constant C is readily found by means of

$$C = (2 + 1/n)(h_{in} - \Delta hA). \quad (73)$$

Combining Eqs. (69) and (73), one gets

$$\sigma(x) = -(1 + 1/n)\Delta h\, x + h_{in} - (2 + 1/n)\Delta hA. \quad (74)$$

In the general case, Eq. (71) is not amenable to analytical solution. We thus consider here the case of constant (pressure-independent) consistency index. Assuming that $\alpha = 0$, Eq. (71) becomes

$$p_{xx} + \frac{n + 1}{x + A}p_x = 0. \quad (75)$$

The solution of the above equation with $p(0) = 1$ and $p(1) = 0$ is

$$p(x) = \frac{\left(\frac{A + 1}{A + x}\right)^n - 1}{(1 + 1/A)^n - 1}. \quad (76)$$

Substituting the pressure into Eq. (72) results in a non-linear algebraic equation which is solved in order to determine the unknown constant A.

For the sake of simplicity, we consider here the case where $g(x) = 1 + x$ (the yield stress varies linearly with the pressure). It is easily shown that Eq. (72) takes the form

$$[\beta Bn + (1 + 1/n)\Delta h]I + (2 + 1/n)\Delta hA = h_{in} - Bn, \quad (77)$$

where

$$I \equiv \int_0^1 pdx = \begin{cases} A\left[(A + 1)\ln(1 + 1/A) - 1\right], & n = 1 \\ \dfrac{(A + 1)(1 + 1/A)^{n-1} - A - n}{(n - 1)\left[(1 + 1/A)^n - 1\right]}, & n \neq 1 \end{cases}. \quad (78)$$

In a linearly converging channel with a slope $\Delta h < 0$, the core thickness increases with a slope equal to $(1 + 1/n)(-\Delta h)$. The value of A can be found analytically only in the two extreme cases between which the lubrication model applies: (a) at the lowest value of Bn, Bn_{c1}, at which the unyielded domain

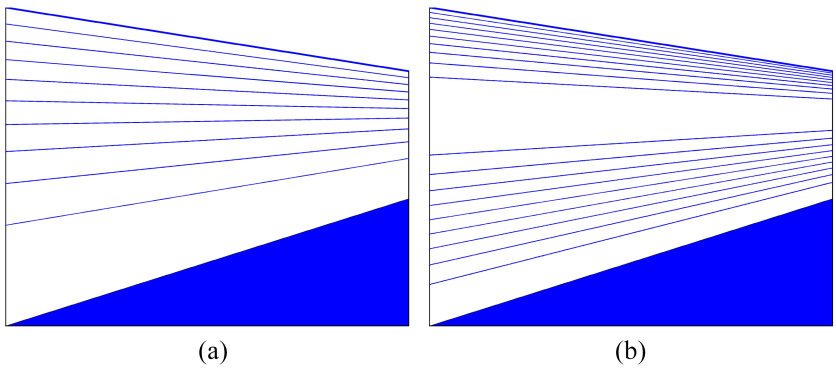

FIG. 9. Velocity contours in the case of the flow of a Bingham plastic ($n = 1$) with constant rheological parameters ($\alpha = \beta = 0$) in a linearly converging channel with $h(x) = 1 - 0.2x$ for $Bn = Bn_{c1} = 0.2594$: (a) v_x and (b) v_y. The unyielded core is shaded, and the contour values are equally spaced.

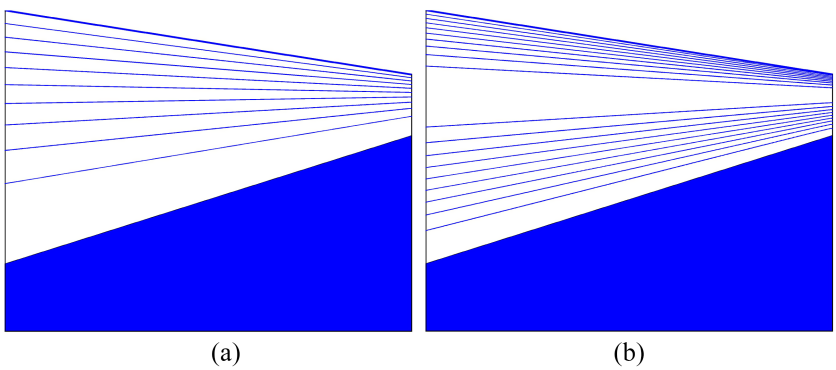

FIG. 10. Velocity contours in the case of the flow of a Bingham plastic ($n = 1$) with constant rheological parameters ($\alpha = \beta = 0$) in a linearly converging channel with $h(x) = 1 - 0.2x$ for $Bn_{c1} < Bn = 0.5 < Bn_{c2}$: (a) v_x and (b) v_y. The unyielded core is shaded, and the contour values are equally spaced.

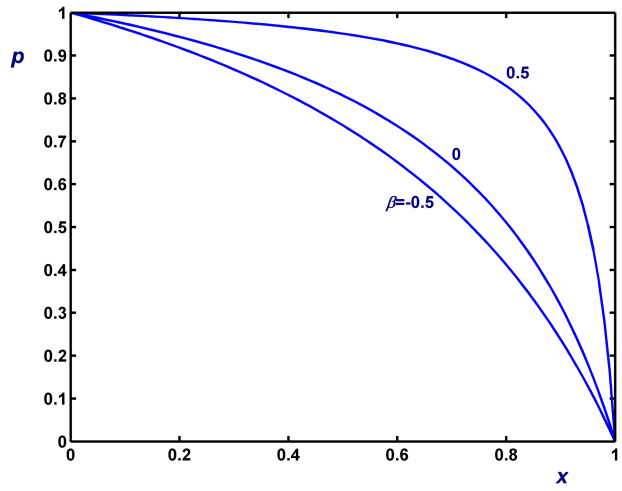

FIG. 11. Effect of the yield-stress growth parameter on the pressure distribution in the case of the flow of a Bingham plastic ($n = 1$) with constant plastic viscosity ($\alpha = 0$) in a linearly converging channel with $h(x) = 1 - 0.2x$ for $Bn = 0.5$; the yield stress is assumed to vary linearly with pressure.

varies from 0 to 1 (it is not broken); (b) at the lowest value of Bn, Bn_{c2}, at which the flow comes to a stop. As illustrated in Fig. 3, for $Bn \geq Bn_{c2}$, there is no flow anyway, while for $Bn < Bn_{c1}$, the plug is broken and the unyielded region is restricted only near the channel exit; the fluid near the inlet is fully yielded and thus the present lubrication model does not apply.

The first critical value Bn_{c1} below which the plug is broken corresponds to $\sigma(0) = 0$. Hence, Eq. (74) yields

$$A = -\frac{h_{in}}{(2 + 1/n)(-\Delta h)},$$

and from Eq. (77), we find that

$$Bn_{c1} = \frac{(1 + 1/n)(-\Delta h)I}{1 + \beta I}. \tag{79}$$

The pressure is given by Eq. (76) and

$$\sigma(x) = -(1 + 1/n)(-\Delta h)x. \tag{80}$$

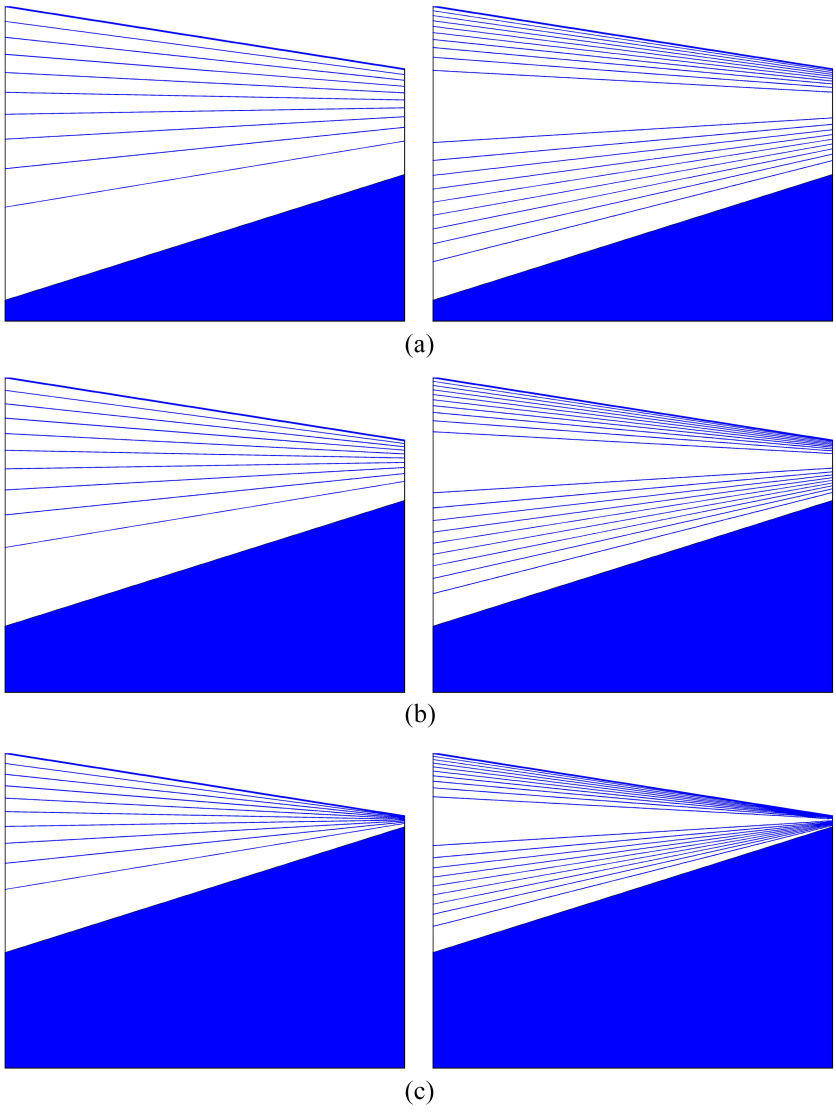

FIG. 12. Effect of the yield-stress growth parameter on the contours of v_x (left) and v_y (right) in the case of the flow of a Bingham plastic ($n = 1$) with constant plastic viscosity ($\alpha = 0$) in a converging channel with $h(x) = 1 - 0.2x$ for $Bn = 0.5$: (a) $\beta = -0.5$; (b) $\beta = 0$; (c) $\beta = 0.5$; the unyielded core is shaded, and the contour values are equally spaced. The yield stress is assumed to vary linearly with pressure.

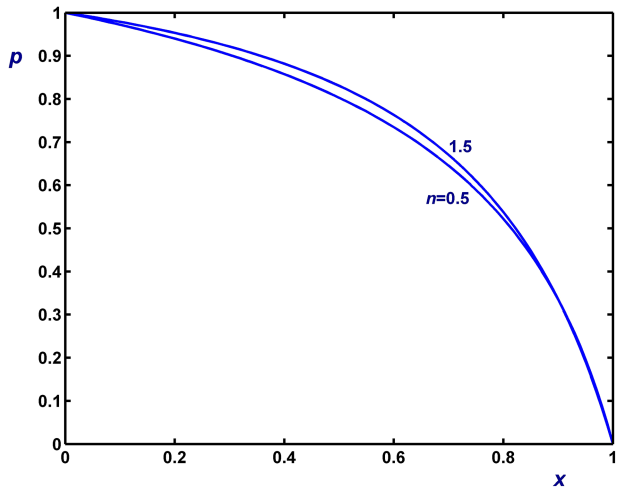

FIG. 13. Effect of the power-law exponent on the pressure distribution in the case of the flow of a Herschel-Bulkley fluid with constant rheological parameters ($\alpha = \beta = 0$) in a converging channel with $h(x) = 1 - 0.2x$ for $Bn = 0.5$.

In general, the second critical value Bn_{c2} is simply that predicted by Eq. (65) for a flat channel of height equal to the minimum value of $h(x)$,

$$Bn_{c2} = \frac{h_{\min}}{1 + \beta/2}, \tag{81}$$

where $h_{\min}$ is the minimum channel height. Hence, for a converging channel,

$$Bn_{c2} = \frac{h_{out}}{1 + \beta/2} = \frac{h_{in} + \Delta h}{1 + \beta/2}. \tag{82}$$

At the critical value Bn_{c2}, the flow stops since $\sigma(1) = h_{in} + \Delta h = h_{out}$. In this case, Eq. (74) gives $A = -1$ and the yield surface is given by

$$\sigma(x) = h_{out} - (1 + 1/n)(-\Delta h)(1 - x). \tag{83}$$

In summary, the method is applicable only when $Bn_{c1} \le Bn \le Bn_{c2}$. When $Bn_{c1} < Bn < Bn_{c2}$, the constant A can be found

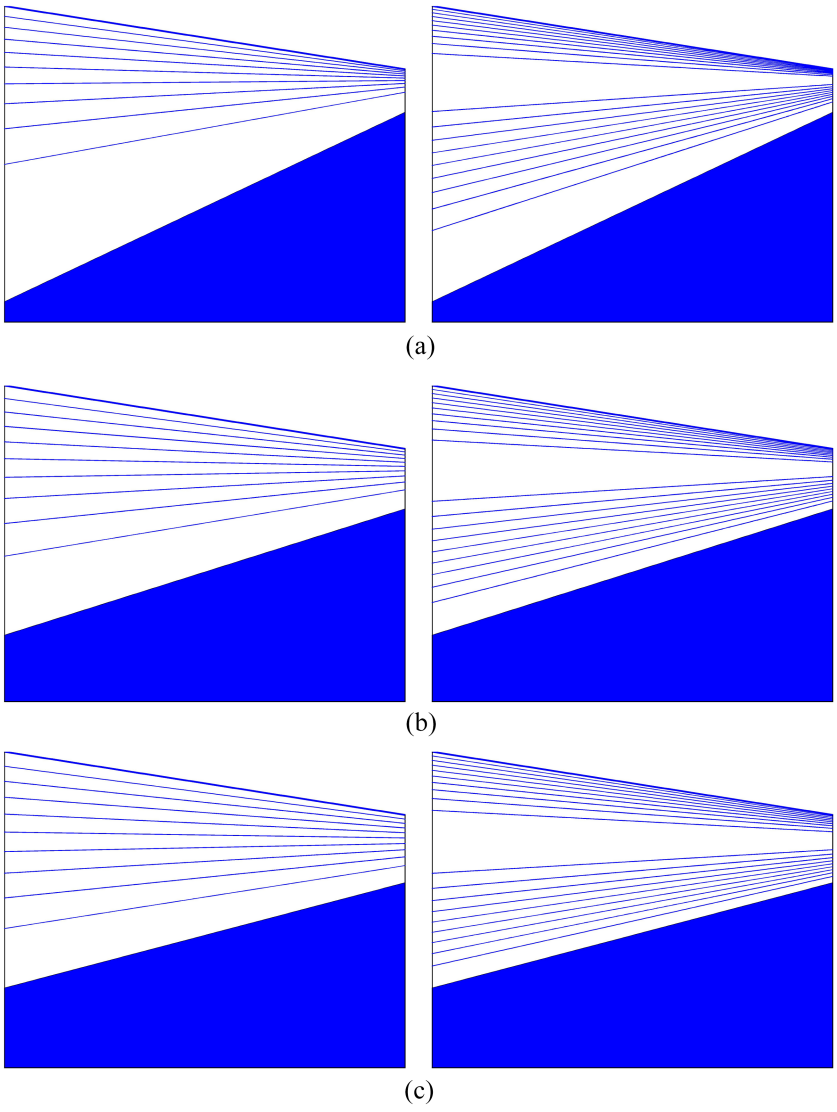

FIG. 14. Effect of the power-law exponent on the contours of v_x (left) and v_y (right) in the case of the flow of a Herschel-Bulkley fluid with constant rheological parameters ($\alpha = \beta = 0$) in a converging channel with $h(x) = 1 - 0.2x$ for $Bn = 0.5$: (a) $n = 0.5$; (b) $n = 1$; (c) $n = 1.5$; the unyielded core is shaded, and the contour values are equally spaced.

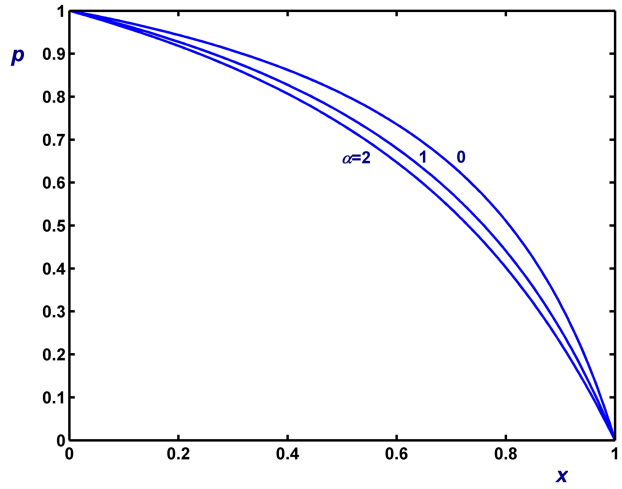

FIG. 15. Effect of the plastic-viscosity growth parameter on the pressure distribution in the case of the flow of a Bingham plastic ($n = 1$) with constant yield stress ($\beta = 0$) in a linearly converging channel with $h(x) = 1 - 0.2x$ for $Bn = 0.5$; the plastic viscosity is assumed to vary linearly with pressure.

numerically as the root of Eq. (77) satisfying

$$-\frac{h_{in}}{(2+1/n)(-\Delta h)} < A < -1. \tag{84}$$

It is obvious that for a given power-law exponent n, Bn_{c2} can be defined only when $\sigma(0) = (2 + 1/n)h_{out} - (1 + 1/n)h_{in} > 0$ or

$$h_{out} > \frac{(1+1/n)}{(2+1/n)}h_{in}. \tag{85}$$

Otherwise, the solution is actually in regime (i); thus, regime (ii) is not observed and the present analysis is not relevant. In other words, the three regimes of Fig. 3 are observed provided that condition (85) is satisfied. Likewise, for a given linearly converging channel, there is a critical value n_c of the power-law exponent below which regime (ii) is not observed,

$$n_c = \frac{(-\Delta h)}{h_{out} + \Delta h}. \tag{86}$$

In the case of a flat channel ($\Delta h = 0$), Bn_{c1} is zero, Bn_{c2} coincides with Bn_c, given by Eq. (65), and the admissible

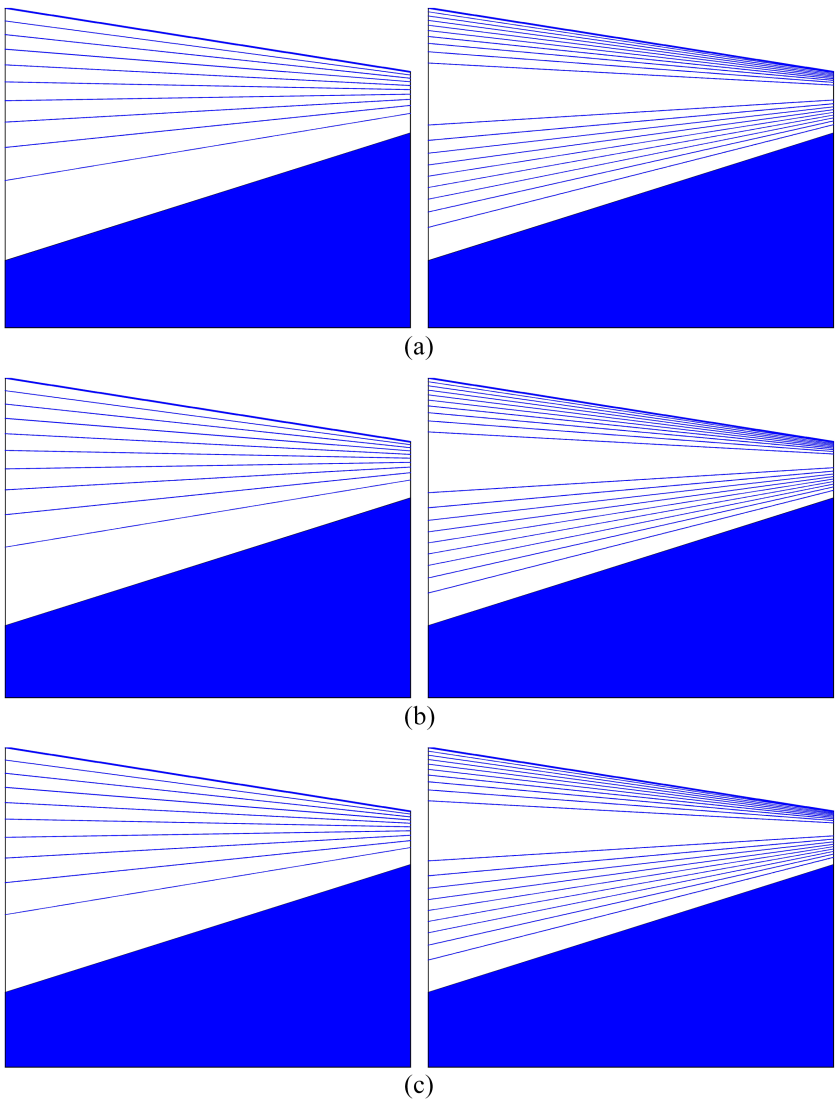

FIG. 16. Effect of the plastic-viscosity growth parameter on the contours of v_x (left) and v_y (right) in the case of the flow of a Bingham plastic ($n = 1$) with constant yield stress ($\beta = 0$) in a converging channel with $h(x) = 1 - 0.2x$ for $Bn = 0.5$: (a) $\alpha = 0$; (b) $\alpha = 1$; (c) $\alpha = 2$; the unyielded core is shaded, and the contour values are equally spaced. The plastic viscosity is assumed to vary linearly with pressure.

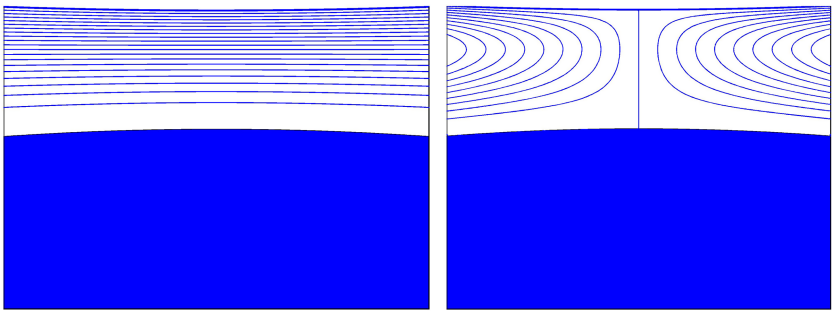

(a) (b)

FIG. 17. Velocity contours in the case of the flow of a Bingham plastic ($n = 1$) with constant rheological parameters ($\alpha = \beta = 0$) in a wavy channel described by Eq. (91) for $Bn = 0.4762$, $\delta = 0.1$ and $\theta = 0.2$: (a) v_x and (b) v_y. The unyielded core is shaded, and the contour values are equally spaced.

values of β are in $[-1, \infty)$. In the case of a linearly varying channel ($\Delta h \neq 0$), the lower bound of β, denoted by β_c, may increase and the applicability of the method is further reduced. This critical value is the maximum of -1 and the value of β at which $Bn_{c1} = Bn_{c2}$. From Eqs. (82) and (79), we then find that

$$\beta_c = \max\left\{-1, 2\frac{[h_{in}/(-\Delta h) - 1]/I - 1 - 1/n}{3 + 1/n - 2h_{in}/(-\Delta h)}\right\}. \tag{87}$$

Figure 4 shows the variation of β_c with $(-\Delta h)$ for $n = 0.5$, 1, and 1.5; β_c is initially -1 and then at a critical value of $(-\Delta h)$ starts increasing to become zero at the maximum admissible value of $(-\Delta h)$, which is determined from Eq. (85),

$$\left.\frac{(-\Delta h)}{h_{in}}\right|_{\max} = \frac{1}{2 + 1/n} \tag{88}$$

(1/4, 1/3, and 3/8 for $n = 0.5$, 1, and 1.5, respectively).

Figures 5–7 illustrate the effect of the yield-stress-growth parameter β on the two critical Bingham numbers for different values of Δh with $h_{in} = 1$ and $n = 0.5$ (shear-thinning), 1 (Bingham plastic), and 1.5 (shear-thickening). The applicability domain of the method corresponds to the shaded regions between the curves of Bn_{c1} and Bn_{c2} (recall that below Bn_{c1} the plug is broken and above Bn_{c2} there is no flow). As $(-\Delta h)$ is increased, this regime is squeezed, with β_c eventually moving to the right; Bn_{c1} increases rapidly, and Bn_{c2} is reduced slightly both tending asymptotically to the curve

$$Bn_c = \frac{1 + 1/n}{(2 + 1/n)(1 + \beta/2)} \tag{89}$$

reached when $(-\Delta h) = 1/(2 + 1/n)$, in which case there is no flow. Comparing Figs. 5–7, we observe that the applicability of the method is increased with n.

The analysis for a linearly diverging channel ($\Delta h > 0$) is analogous. The unyielded core now contracts linearly following Eq. (74). Below a critical Bingham number Bn_{c1}, the unyielded core does not reach the exit plane, and above a second critical number Bn_{c2}, the unyielded core touches the wall at the inlet plane and thus there is no flow. The analysis for the diverging channel holds provided that

$$h_{out} < \frac{2 + 1/n}{1 + 1/n} h_{in}. \tag{90}$$

Let us now consider the flow of a Bingham plastic ($n = 1$) with constant plastic viscosity ($\alpha = 0$) and constant yield stress ($\beta = 0$) in a converging channel with $h(x) = 1 - 0.2x(\Delta h = -0.2)$, in which case $Bn_{c2} = h_{out} = 0.8$. From Eq. (79), we get $Bn_{c1} \simeq 0.2594$. Figure 8 shows the pressure distributions for different values of the Bingham number in the range from Bn_{c1} to Bn_{c2}. Note that when $Bn = Bn_{c2}$ the pressure is equal to unity for $0 \leq x < 1$. The velocity contours for $Bn = Bn_{c1} = 0.2594$ and $Bn = 0.5$ are shown in Figs. 9 and 10, respectively.

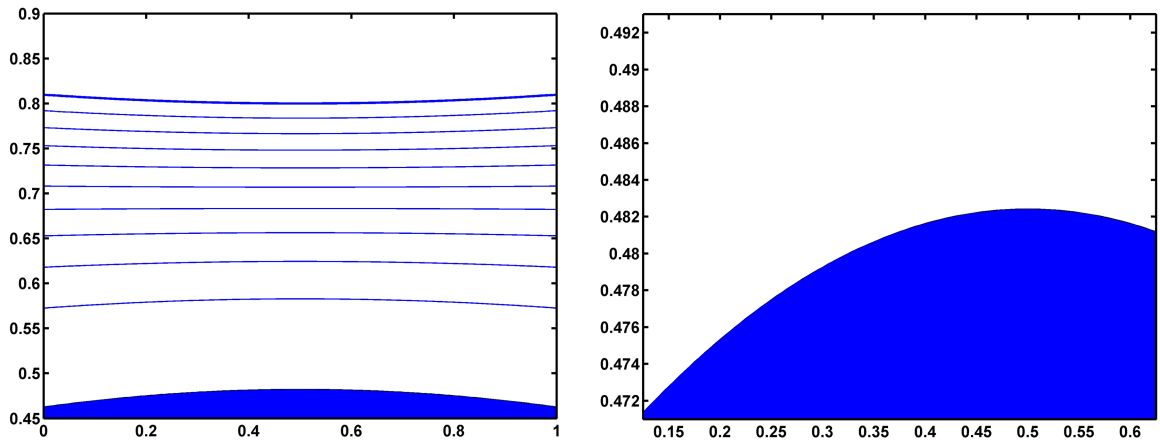

(a) (b)

FIG. 18. Zoomed images of the yielded region in the case of the flow of a Bingham plastic ($n = 1$) with constant rheological parameters ($\alpha = \beta = 0$) in a wavy channel described by Eq. (91) for $Bn = 0.4762$, $\delta = 0.1$ and $\theta = 0.2$ corresponding to Figs. 3 and 4 in Ref. 33: (a) v_x and (b) v_y. The unyielded core is shaded, and the contour values are equally spaced.

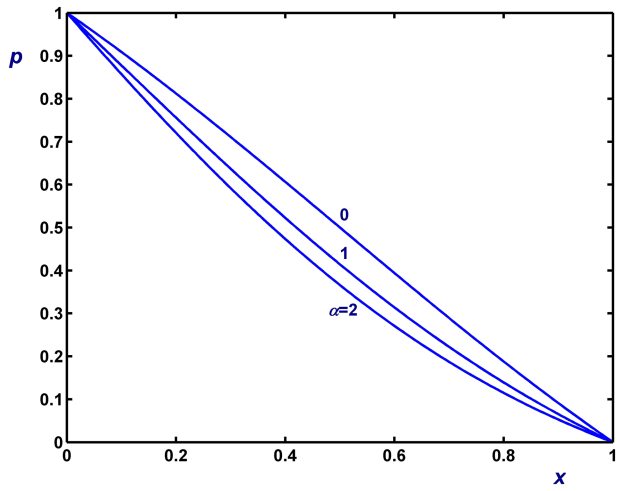

FIG. 19. Effect of the plastic-viscosity growth coefficient on the pressure distribution in the case of the flow of a Bingham plastic (n = 1) with constant yield stress (β = 0) in a wavy channel described by Eq. (91) with Bn = 0.5, δ = 0.1, and θ = 0.2. The plastic viscosity varies linearly with pressure.

The effect of the yield-stress-growth coefficient β on the pressure distribution and the velocity contours is illustrated in Figs. 11 and 12, respectively, which show results for $Bn = 0.5$ and $\beta = -0.5$, 0, and 0.5. The value of the Bingham number was chosen to lie between Bn_{c1} and Bn_{c2} for all the selected values of β (Fig. 11). As β is increased, the dimensionless pressure increases while the pressure gradient becomes lower upstream and higher downstream. As shown in Fig. 12, the slope of the unyielded region remains the same, but this grows bigger as β is increased, reaching the wall at the exit plane when $\beta = \beta_c$ (no flow).

The effect of the power-law exponent in the same geometry ($h(x) = 1 - 0.2x$) can be seen in Figs. 13 and 14, where we show results for n = 1, 0.5, and 1.5 and constant rheological parameters ($\alpha = \beta = 0$). The pressure distribution may be only slightly affected, but the slope of the unyielded region increases as n is reduced. At the critical value $n_c = 1/3$ [Eq. (86)], $\sigma(0) = 0$ and $\sigma(1) = h_{out}$ (thus, the second flow regime where the plug is unbroken is not observed). The material is so shear thinning that the plug hits the wall and no flow occurs.

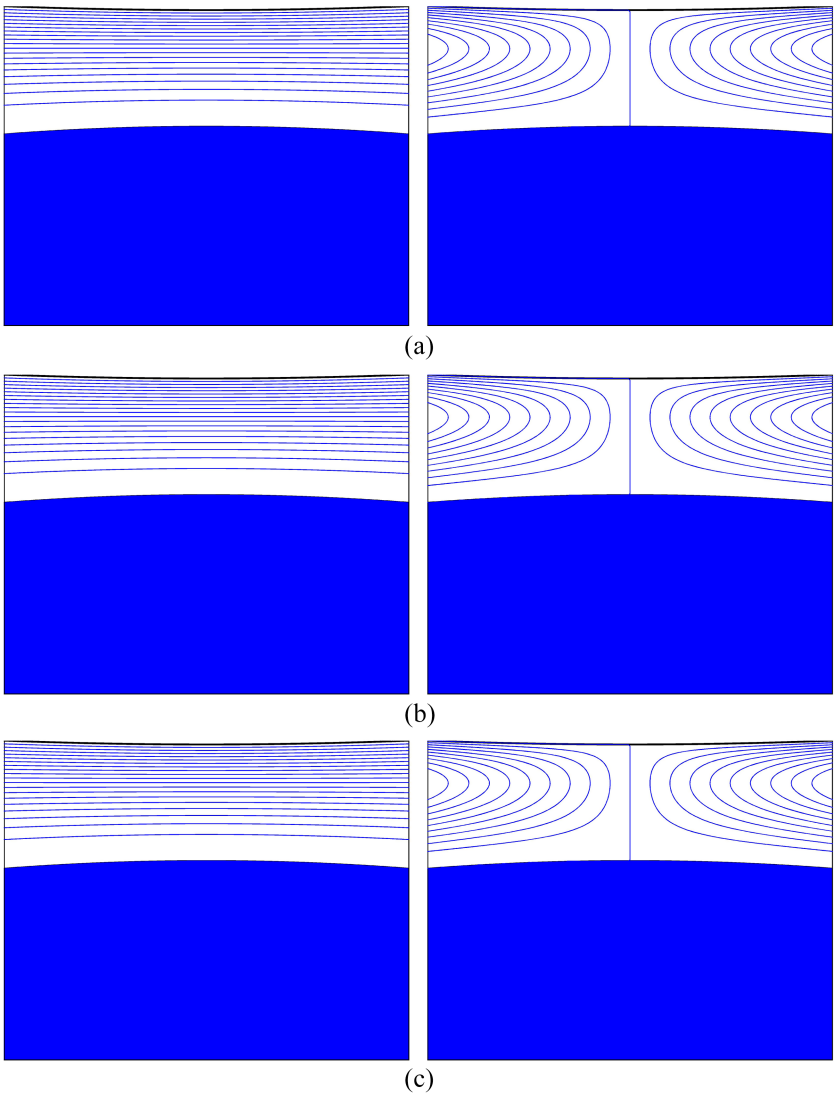

FIG. 20. Effect of the plastic-viscosity growth coefficient on the contours of v_x (left) and v_y (right) in the case of the flow of a Bingham plastic (n = 1) with constant yield stress (β = 0) in a wavy channel described by Eq. (91) with $Bn = 0.5$, $\delta = 0.1$, and $\theta = 0.2$: (a) $\alpha = 0$; (b) α = 1; (c) α = 2; the unyielded core is shaded, and the contour values are equally spaced. The plastic viscosity varies linearly with pressure.

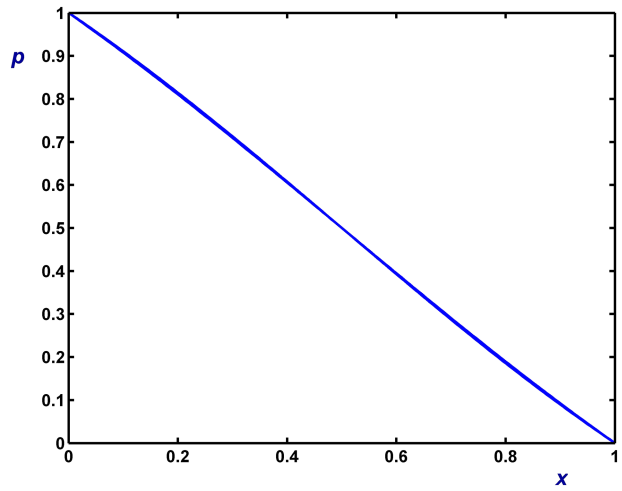

FIG. 21. Effect of the yield-stress growth coefficient on the pressure distribution in the case of the flow of a Bingham plastic ($n = 1$) with constant plastic viscosity ($\alpha = 0$) in a wavy channel described by Eq. (91) with $Bn = 0.5$, $\delta = 0.1$, $\theta = 0.2$, and $\beta = -0.2$, 0 and 2 (the three curves essentially coincide). The yield stress varies linearly with pressure.

We close this section with results for a Bingham plastic ($n = 1$) with constant yield stress ($\beta = 0$) and with plastic viscosity varying linearly with pressure. Since it is not amenable to the analytical solution, this flow is solved numerically using the method briefly described in Sec. V. Figures 15 and 16 show results obtained again in a channel with $h(x) = 1 - 0.2x$ for $Bn = 0.5$ and $\alpha = 0$, 1, and 2. As α is increased, the dimensionless pressure decreases (see Fig. 15), but it should be kept in mind that the applied dimensional pressure driving the flow is increased. The velocity contours for the three values of α are given in Fig. 16. Note that the width of the unyielded region increases with α.

V. FLOW IN A CHANNEL WITH A NONLINEAR WALL FUNCTION

As already mentioned, the integrodifferential equation (49) for the pressure distribution has been solved using a standard pseudo-spectral numerical method.[39] Chebyshev orthogonal polynomials are used to represent the unknown pressure. For each parameter set, the number of spectral

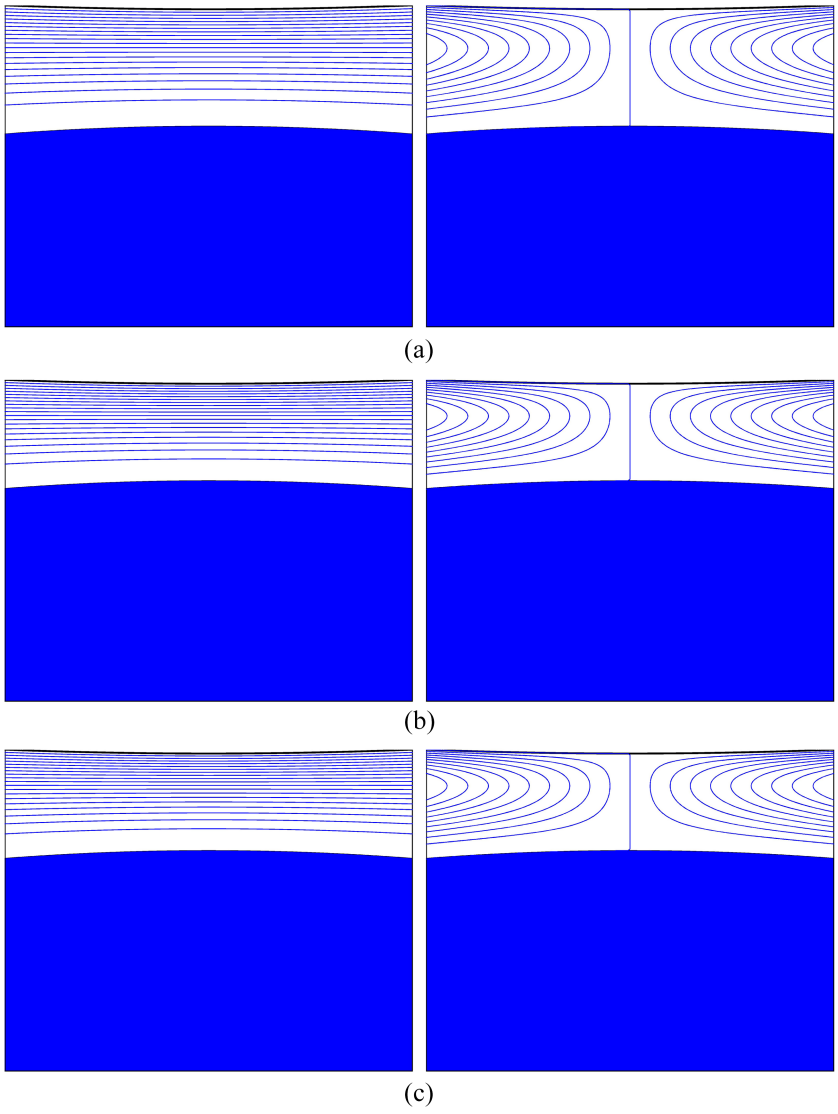

FIG. 22. Effect of the yield-stress growth coefficient on the contours of v_x (left) and v_y (right) in the case of the flow of a Bingham plastic ($n = 1$) with constant plastic viscosity ($\alpha = 0$) in a wavy channel described by Eq. (91) with $Bn = 0.5$, $\delta = 0.1$, and $\theta = 0.2$: (a) $\beta = -0.2$; (b) $\beta = 0$; (c) $\beta = 0.2$; the unyielded core is shaded, and the contour values are equally spaced. The yield stress varies linearly with pressure.

coefficients is adjusted so that a fully resolved pressure field is calculated; 12-18 spectral coefficients are usually required to achieve a decrease in the magnitude of the coefficients about seven to eight orders. To achieve maximum accuracy, all other quantities of interest are also calculated spectrally. Then, the yield surface, unyielded core velocity, and then two velocity components are calculated using the analytical expressions derived in Sec. II.

We considered the wavy channel used by Fusi *et al.*[33] and Frigaard and Ryan,[34]

$$h(x) = 1 - \theta \cos\left[2\pi\delta\left(x - \frac{1}{2}\right)\right], \tag{91}$$

where $\delta > 0$ and $\theta \ll 1$. Figure 17 shows the velocity contours for a Bingham plastic ($n = 1$) with constant rheological parameters ($\alpha = \beta = 0$) obtained with the values chosen in Ref. 33: $Bn = 0.4762$, $\delta = 0.1$, and $\theta = 0.2$. In Fig. 18, we zoom in order to compare with the results of Fusi *et al.*[33] Excellent agreement is observed regarding the shape of the plug region. In all our tests, the contours of v_x were similar to those reported by Fusi *et al.*[33] This was not the case, however, with the v_y contours. Since they intersect the yield surface, the v_y contours of Ref. 33 are in error.

Figures 19 and 20 show respectively the pressure distributions and the velocity contours for the flows of a Bingham plastic ($n = 1$) with constant yield stress ($\beta = 0$) and plastic viscosity varying linearly with pressure when $Bn = 0.5$ and $\alpha = 0$ (constant plastic viscosity), 1, and 2. As before, the dimensionless pressure decreases with α and the pressure gradient increases in magnitude near the inlet and decreases near the exit (Fig. 19). However, as shown in Fig. 20, the elevation of the yield surface is essentially the same (in reality, this increases slightly) and so are the velocity contours.

The results when the yield stress varies linearly with pressure and the plastic viscosity is constant ($\alpha = 0$) seem to follow an opposite trend. Figure 21 shows that the dimensionless pressure distribution is insensitive to β while the width of the unyielded region increases and the velocity contours in Fig. 22 are re-adjusted accordingly. A more careful look on the magnitude of the pressure gradient reveals that this is actually reduced near both the inlet and exit and increases in the middle of the channel as β is increased.

VI. CONCLUSIONS

The flow of a Herschel-Bulkley fluid with pressure-dependent rheological parameters in a channel of varying width has been analyzed extending the lubrication approximation model of Fusi *et al.*[33] for a Bingham plastic ($n = 1$). The zero-order problem in terms of the channel aspect ratio leads to a simple ordinary integro-differential equation for the pressure $p(x)$, which is solved using standard numerical methods (pseudo-spectral method in the present work). Once the pressure is obtained the yield surface and the two velocity components are easily calculated by means of closed-form expressions. Analytical solutions for the special cases of channels of constant and linearly varying regimes have also been obtained.

The present results generalize those of Fusi *et al.*[33] for a Bingham plastic with constant rheological parameters. The lubrication paradox is avoided, and the correct shape of the yield surface is approximated satisfactorily at zero order. The model predicts that at zero order the yield surface variation is opposite to that of the wall multiplied by a factor depending only on the power-law exponent. The pressure dependence of the consistency index and the yield stress affects only the elevation and not the shape of the yield surface. With previous approaches, such a result is obtained only if higher-order solutions are calculated.[34]

A limitation of the method is that it is valid, provided that the unyielded region extends continuously from the inlet to the outlet plane of the channel, i.e., when the plug is not broken. For example, Balmforth and Craster[40] studied the broken-plug regime for the thin-film flow down an inclined plane by means of a consistent thin-layer theory for Bingham plastics. Frigaard and Ryan[34] completed their analysis of viscoplastic flow in a channel of slowly varying width by considering the structure of the flow after the plug was broken. Currently, we investigate the extension of the method to the axisymmetric flow, which is more important in applications.

[1] H. A. Barnes, "The yield stress–a review or 'παντα ρει'–everything flows?," J. Non-Newtonian Fluid Mech. **81**, 133–178 (1999).
[2] N. J. Balmforth, I. A. Frigaard, and G. Ovarlez, "Yielding to stress: Recent developments in viscoplastic fluid mechanics," Annu. Rev. Fluid Mech. **46**, 121–146 (2014).
[3] A. Malkin, V. Kulichikhin, and S. Ilyin, "A modern look on yield stress fluids," Rheol. Acta **56**, 177–188 (2017).
[4] M. Dinkgreve, M. M. Denn, and D. Bonn, "'Everything flows?': Elastic effects on startup flows of yield-stress fluids," Rheol. Acta **56**, 189–194 (2017).
[5] P. Coussot, A. Ya, and G. Ovarlez, "Introduction: Yield stress–or 100 years of rheology," Rheol. Acta **56**, 161–162 (2017).
[6] E. C. Bingham, *Fluidity and Plasticity* (McGraw Hill, New-York, 1922).
[7] W. H. Herschel and R. Bulkley, "Measurement of consistency as applied to rubber-benzene solutions," Am. Soc. Test. Proc. **26**, 621–633 (1926).
[8] E. Mitsoulis and J. Tsamopoulos, "Numerical simulations of complex yield-stress fluid flows," Rheol. Acta **56**, 231–258 (2017).
[9] G. G. Stokes, "On the theories of the internal friction of fluids in motion, and of the equilibrium and motion of elastic solids," Trans. Cambridge Philos. Soc. **8**, 287–305 (1845).
[10] C. Barus, "Isothermals, isopiestics and isometrics relative to viscosity," Amer. J. Sci. **45**, 87–96 (1893).
[11] K. R. Rajagopal, "On implicit constitutive theories for fluids," J. Fluid Mech. **550**, 243–249 (2006).
[12] A. Kalogirou, S. Poyiadji, and G. C. Georgiou, "Incompressible Poiseuille flows of Newtonian liquids with a pressure/dependent viscosity," J. Non-Newtonian Fluid Mech. **166**, 413–419 (2011).
[13] A. Goubert, J. Vermant, P. Moldenaers, A. Göttfert, and B. Ernst, "Comparison of measurement techniques for evaluating the pressure dependence of the viscosity," Appl. Rheol. **11**, 26–37 (2001).
[14] M. M. Denn, *Polymer Melt Processing* (Cambridge University Press, Cambridge, 2008).
[15] C. Venner and A. A. Lubrecht, *Multilevel Methods in Lubrication* (Elsevier, 2000).
[16] M. J. Martín-Alfonso, F. J. Martinez-Bozam, F. J. Navarro, M. Fernández, and C. Gallegos, "Pressure-temperature-viscosity relationship for heavy petroleum fractions," Fuel **86**, 227–233 (2007).
[17] J. Málek and K. R. Rajagopal, "Mathematical properties of the solutions to the equations governing the flow of fluids with pressure and shear rate dependent viscosities," in *Handbook of Mathematical Fluid Dynamics* (Elsevier, 2007).
[18] M. Renardy, "Parallel shear flows of fluids with a pressure-dependent viscosity," J. Non-Newtonian Fluid Mech. **114**, 229–236 (2003).
[19] S. A. Suslov and T. D. Tran, "Revisiting plane Couette-Poiseuille flows of piezo-viscous fluid," J. Non-Newtonian Fluid Mech. **154**, 170–178 (2008).

[20]H. M. Laun, "Pressure dependent viscosity and dissipative heating in capillary rheometry of polymer melts," Rheol. Acta **42**, 295–308 (2003).
[21]J. Hermoso, F. Martinez-Boza, and C. Gallegos, "Influence of viscosity modifier nature and concentration on the viscous behaviour of oil-based drilling fluids at high pressure," Appl. Clay Sci. **87**, 14–21 (2014).
[22]S. O. Osisanya and O. O. Harris, "Evaluation of equivalent circulating density of drilling fluids under high pressure/high temperature conditions," in *SPE 97018, SPE Annual Technical Conference and Exhibition* (Society of Petroleum Engineers, 2005).
[23]C. S. Ibeh, "Investigation on the effects of ultra-high pressure and temperature on the rheological properties of oil-based drilling fluids," M.Sc. thesis, Texas A&M University, 2007.
[24]I. R. Ionescu, A. Mangeney, F. Bouchut, and O. Roche, "Viscoplastic modeling of granular column collapse with pressure-dependent rheology," J. Non-Newtonian Fluid Mech. **219**, 1–18 (2015).
[25]H. C. H. Darley and G. R. Gray, *Composition and Properties of Drilling and Completion Fluids* (Gulf Professional Publishing, Houston, TX, 1988).
[26]M. D. Politte, "Invert oil mud rheology as a function of temperature and pressure," presented at the SPE/IADC Drilling Conference, New Orleans, LA, USA, 6–8 March 1985, SPE Paper No. 13458.
[27]O. H. Houwen and T. Geehan, "Rheology of oil-base muds," in *SPE 15416, SPE Annual Technical Conference and Exhibition* (Society of Petroleum Engineers, New Orleans, 1986).
[28]J. Hermoso, F. Martinez-Boza, and C. Gallegos, "Combined effect of pressure and temperature on the viscous behaviour of all-oil drilling fluids," Oil Gas Sci. Technol.–Rev. IFP Energ. Nouv. **69**, 1283–1296 (2014).
[29]L. Staron, P.-Y. Lagrée, and S. Popinet, "The granular silo as a continuum plastic flows: The hour-glass vs the clepsydra," Phys. Fluids **24**, 103301 (2012).
[30]G. Daviet and F. Bertails-Descourbes, "Nonsmooth simulation of dense granular flows with pressure-dependent yield stress," J. Non-Newtonian Fluid Mech. **234**, 15–35 (2016).
[31]N. L. Khouja, N. Roquet, and B. Cazacliu, "Analysis of a regularized Bingham model with pressure-dependent yield stress," J. Math. Fluid Mech. **17**, 723–739 (2015).
[32]L. Fusi, "Non-isothermal flow of a Bingham fluid with pressure and temperature dependent viscosity," Meccanica **52**, 3577–3592 (2017).
[33]L. Fusi, A. Farina, F. Ross, and S. Roscani, "Pressure-driven lubrication flow of a Bingham fluid in a channel: A novel approach," J. Non-Newtonian Fluid Mech. **221**, 66–75 (2015).
[34]I. A. Frigaard and D. P. Ryan, "Flow of a visco-plastic fluid in a channel of slowly varying width," J. Non-Newtonian Fluid Mech. **123**, 67–83 (2004).
[35]A. Putz, I. A. Frigaard, and D. M. Martinez, "On the lubrication paradox and the use of regularization methods for lubrication flows," J. Non-Newtonian Fluid Mech. **163**, 62–77 (2009).
[36]L. Fusi, A. Farina, and F. Rosso, "Bingham flows with pressure-dependent rheological parameters," Int. J. Non-Linear Mech. **64**, 33–38 (2014).
[37]Y. Damianou and G. C. Georgiou, "On Poiseuille flows of a Bingham plastic with pressure-dependent rheological parameters," J. Non-Newtonian Fluid Mech. **250**, 1–7 (2017).
[38]L. Fusi and F. Rosso, "Creeping flow of a Herschel-Bulkley fluid with pressure-dependent material moduli," Eur. J. Appl. Math. (in press).
[39]J. S. Hesthaven, S. Gottlieb, and D. Gottlieb, *Spectral Methods for Time-Dependent Problems* (Cambridge University Press, Cambridge, 2007).
[40]N. J. Balmforth and R. V. Craster, "A consistent thin-layer theory for Bingham plastics," J. Non-Newtonian Fluid Mech. **84**, 65–81 (1999).